catalysts

MDPI

Review

Dielectric Barrier Discharge Plasma Coupled with Catalysis for Organic Wastewater Treatment: A Review

He Guo [1], Yingying Su [1], Xinyi Yang [2], Yawen Wang [1], Zhen Li [1], Yifeng Wu [3,*] and Jingyu Ren [2,*]

[1] College of Biology and the Environment, Nanjing Forestry University, Nanjing 210037, China
[2] School of Petroleum Engineering and Environmental Engineering, Yan'an University, Yan'an 716000, China
[3] School of Energy and Environment, Southeast University, Nanjing 210096, China
* Correspondence: 101011433@seu.edu.cn (Y.W.); renjingyuyau@163.com (J.R.)

Abstract: Dielectric barrier discharge (DBD) plasma in advanced oxidation technology can degrade organic pollutants in water under mild conditions. It has the advantages of universality, simple reaction conditions, and no secondary pollution. However, the light, electrons, and low-reactive substances generated during the discharge process cannot be fully utilized, which limits the further application of DBD plasma. Therefore, the DBD system coupled with catalysis can not only solve the above problem, but also transforms the low-active substances into high-active substances and improves the degradation rate of organic pollutants. Based on this fact, this review focuses on the characteristics and principles of DBD plasma coupled with photocatalysis, adsorption, Fenton oxidation, persulfate oxidation and composite technology to treat organic wastewater. This review puts forward some problems of DBD synergetic catalysis technology, and looks forward to the future development direction of this technology to treat organic pollutants in water.

Keywords: dielectric barrier discharge; plasma; catalysis; organic; wastewater treatment

Citation: Guo, H.; Su, Y.; Yang, X.; Wang, Y.; Li, Z.; Wu, Y.; Ren, J. Dielectric Barrier Discharge Plasma Coupled with Catalysis for Organic Wastewater Treatment: A Review. *Catalysts* **2023**, *13*, 10. https://doi.org/10.3390/catal13010010

Academic Editor: Enric Brillas

Received: 27 November 2022
Revised: 20 December 2022
Accepted: 21 December 2022
Published: 22 December 2022

1. Introduction

In recent years, with the rapid development of industrialization and urbanization in countries around the world, the discharge of various forms wastewater has also increased. Many chemical plants and hospitals have discharged a large amount of wastewater containing various refractory organic pollutants, such as organic pesticides [1], phenols [2], antibiotics [3] and dyes [4,5]. These refractory organic pollutants have the characteristics of high toxicity and easy accumulation in organisms. Their long-term residue in the water environment can seriously affect the stability of ecosystems and endanger human health [6]. Therefore, it is urgent to solve the water pollution problem.

In recent years, a large number of scholars have made many contributions to organic wastewater treatment. There are three traditional water pollution treatment methods: the physical method, chemical method and biological method [7]. Physical methods mainly include membrane separation [8], air floatation [9] and adsorption [10,11], etc. They are often used as the primary treatment of wastewater to remove part of the suspended substances in wastewater. It has the advantages of easy availability of raw materials and low price, but it also has disadvantages such as application limitations and low COD removal rate [12]. The chemical method refers to adding chemical flocculants or chemical oxidants to wastewater to remove pollutants in wastewater. This method degrades pollutants in a short time, but it also produces sludge and degradation by-products, causing secondary pollution to the water environment [13]. The biological method mainly includes aerobic biological treatment and anaerobic biological treatment, which has low cost and can be flexibly applied to various water qualities, but it also has the problem of a too-long treatment cycle [14]. The wastewater from chemical plants and hospitals contains a large number of organic pollutants which are difficult to be degraded and cannot be effectively treated by

traditional sewage treatment methods. More green and efficient technologies are needed to degrade organic pollutants in wastewater.

Advanced oxidation processes (AOPs) have high degradation rate of organic pollutant, stable catalytic efficiency, and no secondary pollution [15], so they have attracted more and more attention in water pollution treatment. AOPs mainly relies on the generation of strong oxidizing group ·OH to efficiently degrade organic pollutants in water. It mainly includes the Fenton oxidation method [16], ozone oxidation method [17], photocatalytic method [18], electrochemical method [19], ultrasonic oxidation method [20], persulfate oxidation [21], etc. As one of the AOPs, dielectric barrier discharge (DBD) plasma technology is a composite advanced oxidation technology integrating ozone oxidation, photocatalysis and ultrasonic oxidation [22], which has a fast reaction speed, high degradation efficiency, and no secondary pollution. In the process of discharge, DBD dissociates gas and water molecules to produce a large number of active free radicals, and also radiates ultraviolet light, shock waves and other physical effects, which can remove a variety of refractory organic pollutants. However, the ultraviolet light, electrons and various active substances produced in the discharge process cannot be fully utilized, resulting in the low energy utilization rate of a DBD system. Therefore, it is considered to combine DBD plasma with other catalytic technologies, which can not only improve the utilization rate of electron and light energy, and accelerate and promote the generation of active substances, but also further improve the degradation rate of pollutants.

In recent years, research on DBD plasma technology has been widely used in water pollution treatment and water remediation. However, there have been few reviews on DBD plasma co-catalytic technology. In addition, the mechanism and degradation process of DBD plasma-catalyzed degradation of organic pollutants are still unclear. According to the classification shown in Figure 1, this paper reviews the degradation of organic pollutants in water by DBD plasma combined with other typical catalysis technologies (photocatalysis, adsorption catalysis, Fenton catalysis, and persulfate catalysis). In this paper, DBD plasma technology is introduced first, and then several methods of collaborative catalytic degradation of organic pollutants by DBD plasma technology are summarized and their advantages and disadvantages are expounded. In addition, the mechanism of various DBD plasma co-catalytic technologies and the influence of various factors on the degradation rate of organic matter are described. The energy efficiency and degradation pathways of typical DBD plasma co-catalytic techniques are further compared. Finally, the paper forms a summary and puts forward the prospect for the future.

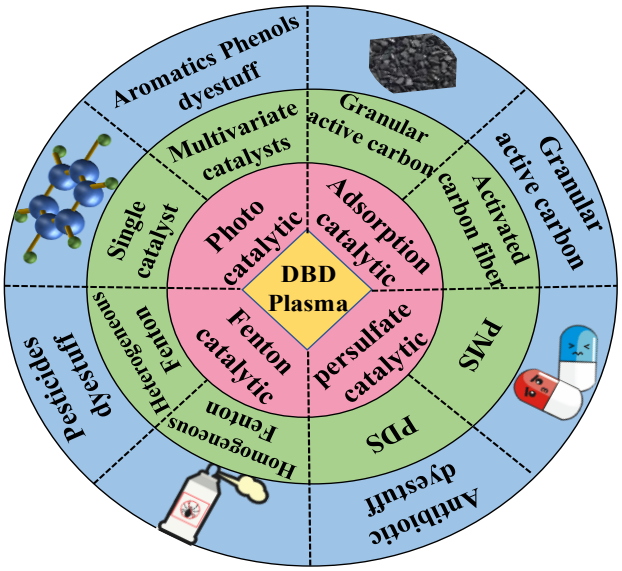

Figure 1. Classification of DBD plasmas coupled to other catalysts.

2. DBD Water Treatment Technology

Plasma was first proposed by Tonks and Langmuir in 1929 and endowed with the meaning of "ionized gas". It is mainly composed of active substances such as electrons, ions and free radicals. It is divided into thermal plasma and non-thermal plasma (NTP) [23]. NTP is usually produced by gas discharge, which can be divided into the following types according to different discharge forms: DBD [24], corona discharge [25], sliding arc discharge [26], glow discharge [27] and pulse discharge [28], etc. NTP also has a variety of functions such as high-energy electrons, ozone oxidation and ultraviolet radiation, and has a significant degradation effect on the treatment of organic pollutants in water [29]. DBD, as a kind of NTP, is often used in the treatment of organic wastewater.

DBD is a non-equilibrium gas discharge with an insulating medium inserted into the discharge space [30,31]. The insulating medium usually consists of quartz, glass and ceramics. Different DBD reactors have different experimental results. Figure 2 shows the water treatment reactors using jet-type DBD [32], coaxial-type [33], falling-film-type [34] and plate-type [35] by different researchers. The existence of insulating medium can avoid the formation of arc lights and sparks, so that the discharge is more uniform and stable. In the process of discharge, active groups such as H_2O_2, O_3 and ·OH will be generated, and physical effects such as high-energy electrons, ultraviolet radiation, local high temperature and shock waves will also occur [36].

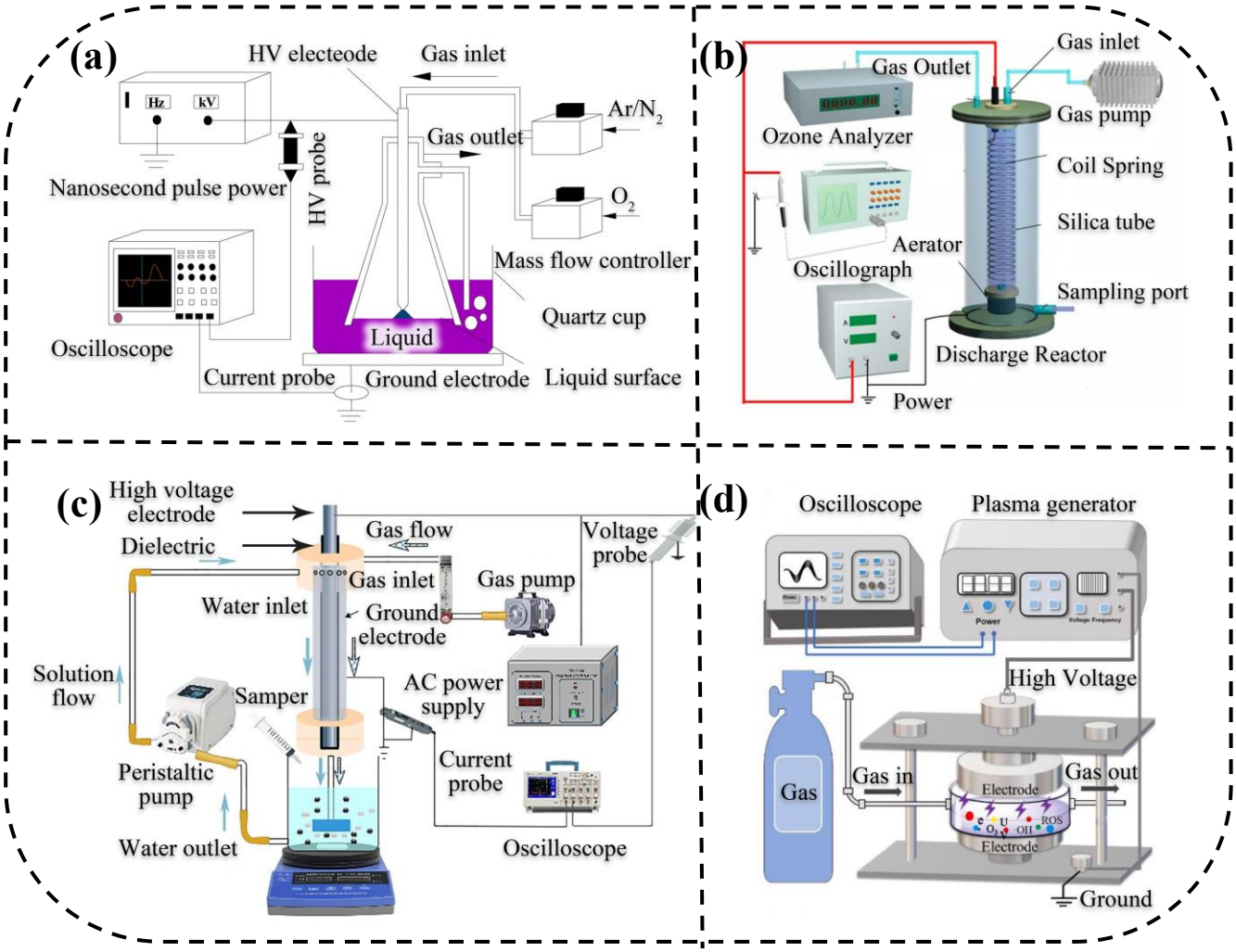

Figure 2. Structure chart of various DBD reactors: (**a**) Structure chart of jet DBD system reactor [32]; (**b**) Structure chart of coaxial DBD system reactor [33]; (**c**) Structure chart of falling-film DBD system reactor [33]; (**d**) Structure chart of plate–plate DBD system reactor [35].

A DBD system can act on organic pollutants in water through active groups and physical effects, and has the characteristics of a simple reactor structure and high treatment efficiency. Therefore, the DBD system has become a research highlight of wastewater treatment in recent years. Hu [37], Kil [38] and Sahu [39] used a DBD system to degrade pefloxacin (PEF), sulfathiazole and phenol, respectively, and their degradation rates were as high as 96.1%, 100.0% and 98.0%. In addition, the number of documents retrieved from 2010 to 2022 on the Web of Science (WOS) and China National Knowledge Infrastructure (CNKI) with the theme of "Dielectric Barrier Discharge" and "Wastewater Treatment" is shown in Figure 3. As can be seen from Figure 3, the DBD system, as a new technology, has attracted extensive attention from researchers in recent years, especially in the past five years. The methods of wastewater treatment by various DBD systems have developed rapidly, and the scientific research achievements have been quite abundant. The DBD system is expected to be an important alternative to traditional chemical process.

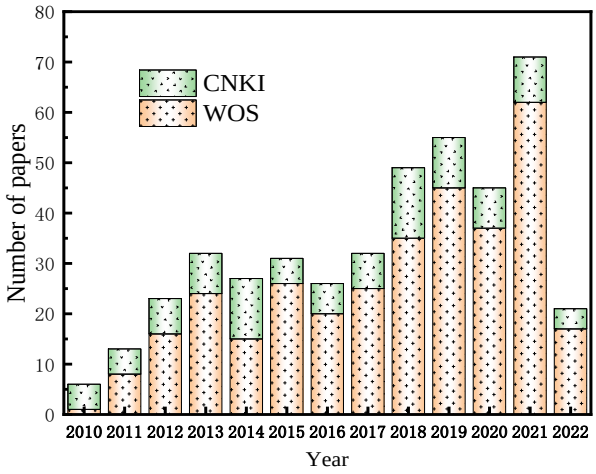

Figure 3. The number of literature sources related to wastewater treatment by DBD from 2010 to 2022.

However, there are also some problems when using a separate DBD system to treat wastewater, such as high energy consumption, poor energy utilization and low mineralization. Therefore, the DBD system needs to cooperate with other catalytic methods to degrade organic wastewater [40]. Figure 4 shows the proportion of literature sources related to different DBD co-catalytic methods in CNKI and WOS. These typical DBD synergistic catalysis methods are mainly expounded below.

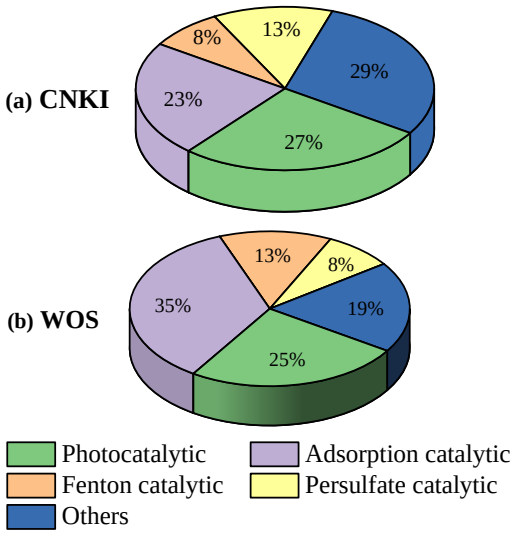

Figure 4. The percentage of various DBD collaborative catalytic methods in (**a**): CNKI; (**b**): WOS.

3. DBD Coupled with Catalysis

3.1. DBD Coupled with Photocatalysis

Photocatalysis belongs to advanced oxidation technology. Common photocatalysts include TiO_2, ZnO, CdS and other semiconductor materials [41]. Among them, TiO_2 is widely used due to its good catalytic effect, no secondary pollution, non-toxicity and low cost [42]. The action mechanism of TiO_2 is as follows: when it is irradiated by light with energy exceeding its band gap width, electrons will be excited from the valence band to the conduction band, thus forming a highly reductive electron (e^-) in the conduction band, and at the same time producing a highly oxidizing hole (h^+) in the valence band [43]. The h^+ can react with H_2O and OH^- to produce ·OH with stronger oxidation; e^- can react with O_2 to generate $\cdot O_2^-$, and further generate H_2O_2. The main reaction equation is shown in Equations (1)–(6) [44,45]:

$$TiO_2 + hv \rightarrow TiO_2 + e^- + h^+ \quad (1)$$

$$h^+ + H_2O \rightarrow \cdot OH + H^+ \quad (2)$$

$$h^+ + OH^- \rightarrow \cdot OH \quad (3)$$

$$e^- + O_2 \rightarrow \cdot O_2^- \quad (4)$$

$$\cdot O_2^- + H^+ \rightarrow HO_2\cdot \quad (5)$$

$$2HO_2\cdot \rightarrow H_2O_2 + O_2 \quad (6)$$

Aiming at the problem that most of the UV light generated during DBD plasma discharge does not participate in the degradation process of pollutants [46], DBD plasma can be coupled to a photocatalyst to improve the utilization rate of UV light. Moreover, the e^- and h^+ formed by the photocatalyst act on H_2O and O_2, respectively, to form strong oxidizing free radicals ·OH and $\cdot O_2^-$, which further accelerate the process of oxidation and decomposition of organic pollutants. The degradation mechanism of a DBD system combined with a typical photocatalyst TiO_2 is shown in Figure 5 [47]:

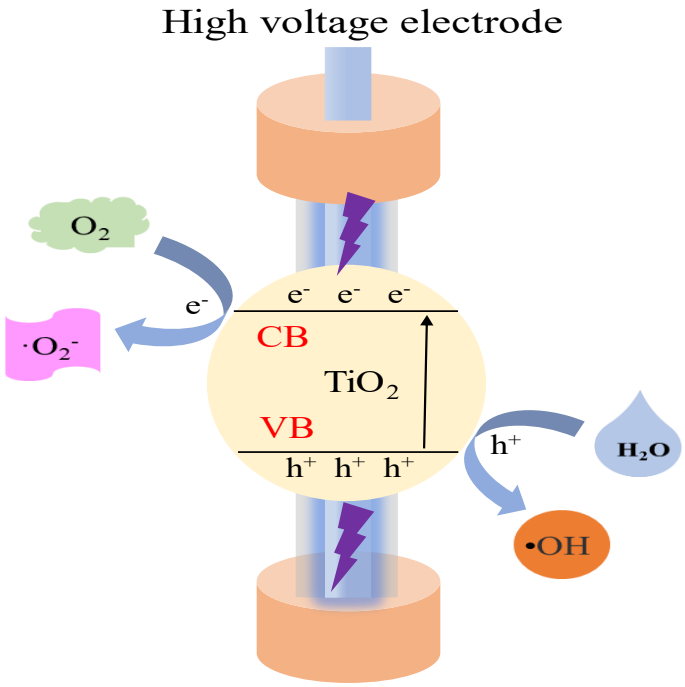

Figure 5. Mechanism of DBD coupled with TiO_2 for the degradation of organic pollutants.

Table 1 summarizes the research of some domestic and foreign scholars using a DBD system in collaboration with a photocatalyst to degrade organic pollutants in water [48–54].

It can be found that the final removal rate of target pollutants can reach almost 80.0–90.0% when TiO_2 is widely used as the photocatalyst. In addition, the shock wave generated by the DBD system during the discharge process can clean the surface of the photocatalyst and increase the active sites on the surface of the photocatalyst, thus enhancing the catalytic degradation efficiency. However, the dosage of the photocatalyst should not be too much. Excess photocatalyst would increase the turbidity of solution, reduce the ability of photocatalyst to absorb ultraviolet light, and eventually reduce the degradation rate of the pollutants.

Table 1. Energy efficiency and synergetic factor.

Researchers	Target Pollutant	Photocatalyst	Experimental Conditions	Degradation Rate	Ref.
Tijani et al.	2-NP	load type of TiO_2	Discharge voltage: 8.0 kV; Air flow rate: 3.0 L/min; 2-NP concentration: 10.0 PPM; Time: 60.0 min	77.5%	[48]
Li et al.	2,4-dichlorophenol	TiO_2	Discharge voltage: 75.0 V; 2,4-dichlorophenol concentration: 50.0 mg/L; pH: 5.3; TiO_2 supplemental amount: 10%; Time: 120.0 min	89.6%	[49]
Li et al.	Clothianidin	rGO/TiO_2	Applied power: 200 W; Clothianidin concentration: 0.1 g/L; pH: 3.5; Electrical conductivity: 150.0 S/cm; Time: 120.0 min	98.9%	[50]
Tao et al.	Methyl orange (MO)	ZnCuFeCr	Input voltage:30.9 kV; MO concentration: 20.0 mg/L; ZnCuFeCr dosage: 1.0 g/L; Time: 42.0 min	96.8%	[51]
Zheng et al.	MO	Ce/Mo	Input voltage: 3.6 kV; MO concentration: 50.0 mg/L; Time: 18.0 min	80.0%	[52]
Tao et al.	MO	Modified NiAlCe-LDH	Input voltage: 70.0 V; MO concentration: 80.0 mg/L; Modified NiAlCe-LDH dosage: 1.0 g/L; Time: 36.0 min	100.0%	[53]
Liu et al.	Acid orange 7(AO7)	g-C_3N_4/TiO_2	Input power: 20.0 W; AO7 concentration: 5.0 mg/L; Air flow rate: 52.0 L/h; pH: 10.0; Catalyst dosage: 0.5 g/L; Time: 10.0 min	100.0%	[54]

Different photocatalysts have different catalytic mechanisms and degradation effects on pollutants in different pH solutions. Under the optimum acid–base conditions, the degradation rate of DBD synergetic photocatalysis is the highest. Li et al. [49] also made the same finding in their study on the degradation of clothianidin by DBD plasma in collaboration with rGO-TiO_2: the reactions of H_2O_2 at different acidity and alkalinity were different. H_2O_2 was more likely to be converted into ·OH under acidic conditions, and more likely to be converted into HO_2· with less oxidizing than ·OH under alkaline conditions. Therefore, acidic conditions are more conducive to pollutant degradation.

3.2. DBD Coupled with Adsorption Catalysis

The adsorption method refers to the method of adding adsorbent with a dense porous structure into wastewater to separate and enrich pollutants through physical or chemical action [55]. The adsorption method has the advantages of simple operation and low investment cost. The dense porous structure and huge specific surface area of the adsorbent enable it to have strong adsorption capacity [11]. In addition, the active groups on the adsorbent surface can also form chemical bonds with the adsorbate to selectively adsorb organic pollutants in water [56]. At present, the commonly used adsorbents include ion exchange resin [57], activated carbon (AC) [58] and zeolite molecular sieves [59]. AC is an adsorbent with extremely rich pores. Its surface has oxygenated functional groups that can adsorb organic pollutants in water. It mainly relies on electrostatic force and ion exchange to adsorb pollutants [60].

However, adsorption saturation exists in the adsorbent, and the effect of treating organic matter in water will be greatly reduced after adsorption saturation [61]. When

a single DBD system is used to treat low-concentration organic wastewater, the strong oxidizing groups generated by DBD are difficult to react directly with organic substances in water, resulting in a poor treatment effect. Therefore, the DBD system can be combined with the adsorption method. Firstly, the adsorbent adsorbed organic pollutants in wastewater on its surface, and the high-energy electrons, reactive free radicals, and various physical effects of the DBD system rapidly degraded the adsorbed organic pollutants. Secondly, DBD degraded the pollutants adsorbed between the pores of the adsorbent and released the adsorption sites on the adsorbent, so that the adsorbent recovered the adsorption function and the adsorbent was regenerated [62]. Figure 6 shows the mechanism diagram of the DBD coupling with the typical adsorption catalyst (AC).

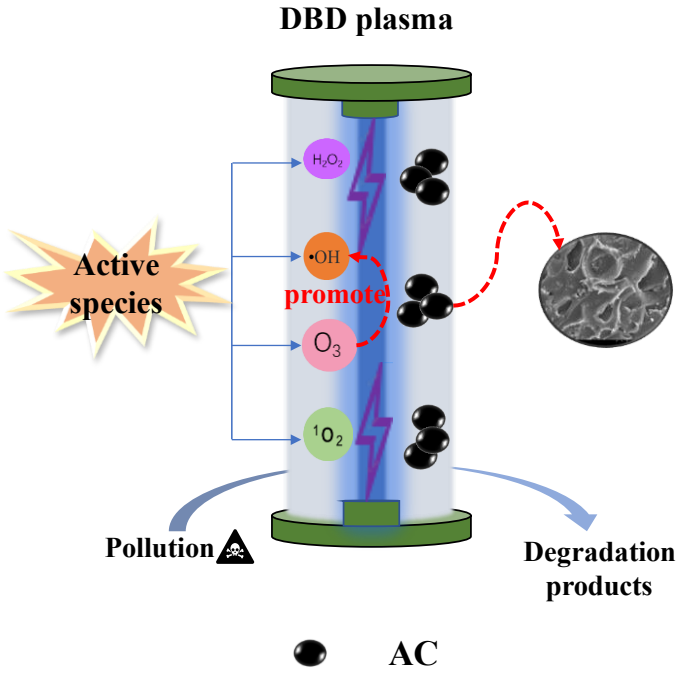

Figure 6. Mechanism of DBD coupled with AC for the degradation of organic pollutants.

Table 2 summarizes the studies of some scholars on the degradation of organic pollutants in water by using a DBD system in coordination with adsorption catalyst [63–68]. It can be found that AC is the main adsorbent. In order to improve the adsorption capacity of AC, the AC was improved, such as activated carbon fiber (ACFs), granular activated carbon (GAC) and loaded activated carbon. When the DBD system cooperates with the AC for adsorption and catalysis, the AC plays two roles. One is adsorption, which adsorbs organic pollutants onto its surface, and the DBD system reprocesses. The second is catalysis; the DBD system generates O_3 during discharge, and the AC can react with O_3 to form ·OH. The reaction process is as follows (as Equations (7)–(13)) [63,66]:

$$O_3 + \text{H-AC-H} \rightarrow \text{AC-O} + H_2O_2 \quad (7)$$

$$O_3 + \text{AC-OH} \rightarrow \cdot O_2\text{-AC} + \cdot\text{OH} \quad (8)$$

$$O_3\text{-AC} \rightarrow O_2 + \cdot\text{O-AC} \quad (9)$$

$$O_3 + \cdot\text{O-AC} \rightarrow \cdot O_2 + \text{O} + \text{AC} \quad (10)$$

$$\text{AC} + \text{M} \rightarrow \text{AC}\cdots\text{M} \quad (11)$$

$$\text{AC}\cdots\text{M} + \cdot\text{OH} \rightarrow \text{AC} + \text{Intermediate products} \quad (12)$$

$$\text{Intermediate products} + \cdot\text{OH} \rightarrow CO_2 + H_2O \quad (13)$$

Table 2. Summary of DBD technologies with adsorption for the organic wastewater removal.

Researchers	Target Pollutant	Adsorbent	Experimental Conditions	Degradation Rate	Ref.
Gushchin et al.	2,4-dichlorophenol (2,4-DCP)	diatomite	Discharge power: 1.8 W; Time: 2.5 s	~92.0%	[63]
Sang et al.	N, N-dimethylformamide (DMF)	Mn-AC	Discharge power: 16.2 W; DMF concentration: 100.0 mg/L; pH: 11.4; Mn-AC dosage: 1.0 g/L; Time: 40.0 min	82.2%	[64]
Gong et al.	Levofloxacin (LFX)	Ag_3PO4/ACFs	Discharge voltage: 10.0 kV; LFX concentration: 20.0 mg/L; Time: 18.0 min	93.0%	[65]
Lu et al.	Pentachlorophenol (PCP)	GAC	Discharge voltage: 23.0 kV; Concentration of PCP: 2000.0 mg/L; Air flow: 2.0 L/min; Time: 2.0 h	65.0%	[66]
Qu et al.	PCP	GAC	Discharge voltage: 20.4 kV; Frequency: 200.0 Hz; PCP concentration: 2000.0 mg/L; Oxygen flow: 2.0 L/min; Time: 60.0 min	67.0%	[67]
Tang et al.	Phenol	GAC	Discharge voltage: 21.0 kV; Air flow: 0.45 m^3/h; Time: 60.0 min	58.0%	[68]

The DBD system can regenerate the AC to a certain extent, but the average pore diameter of the AC after DBD treatment is larger than that of the original AC, and the adsorption capacity of the reactivated carbon is not as good as that of the original state [67,68]. The active groups on the surface of the adsorbent oxidized, which resulted in the expansion of the original pores or the generation of new pores. The physical and chemical effects of the DBD system made the pores collapse. In addition, part of the organic pollutants that were not degraded were adsorbed between pores, which caused pore blockage.

3.3. DBD Coupled with Fenton Oxidation Catalysis

The principle of the Fenton oxidation process is that Fe^{2+} and H_2O_2 react to produce highly oxidizing ·OH (as Equation (14)), which is suitable for the treatment of organic wastewater that is difficult to be biodegraded [69,70].

$$Fe^{2+} + H_2O_2 \rightarrow Fe^{3+} + OH^- + \cdot OH \quad (14)$$

$$Fe^{2+} + \cdot OH \rightarrow Fe^{3+} + OH^- \quad (15)$$

$$Fe^{3+} + H_2O_2 \rightarrow Fe^{2+} + HO_2\cdot + H^+ \quad (16)$$

$$Fe^{3+} + UV + H_2O \rightarrow Fe^{2+} + \cdot OH + H^+ \quad (17)$$

The Fenton oxidation process has strong oxidation capacity and a fast reaction, and can effectively treat organic wastewater. However, there are still some problems when Fenton oxidation is used alone. First of all, the utilization rate of H_2O_2 is not high [71], so a large amount of H_2O_2 is needed to maintain the continuation of the reaction, which leads to a large increase in the cost of wastewater treatment. Secondly, a certain concentration of Fe^{2+} is conducive to the degradation of pollutants, while excessive Fe^{2+} will react with ·OH (as Equation (15)), thus reducing the concentration of ·OH in water and the degradation rate of target pollutants. Although Fe^{3+} can be converted to Fe^{2+} under certain conditions, the addition of Fe^{2+} and DBD system is usually selected to form a co-catalytic condition. The reason is that a large amount of H_2O_2 is consumed during the conversion of Fe^{3+} to Fe^{2+}, which greatly reduces the content of H_2O_2 produced by the DBD system and thus reduces the content of ·OH generated by the reaction with Fe^{2+}. The specific reaction equation is shown in Equation (16) [70]. In order to improve the treatment of organic pollutants in water by the Fenton oxidation process, the photo-Fenton method [72], electro-Fenton method [73], ultrasound-Fenton method [74], etc., were proposed.

The DBD system will produce H_2O_2 in the process of wastewater treatment, so the DBD system can be used to cooperate with the Fenton oxidation method to degrade organic pollutants, improve the utilization rate of H_2O_2 in the DBD system, and reduce the cost of adding H_2O_2. In addition, the DBD system will generate ultraviolet light in the reaction

process, and the Fenton oxidation method can combine with ultraviolet light [75] to generate more ·OH. Fe^{3+} can be reduced under the action of ultraviolet light to regenerate Fe^{2+} and improve the recycling efficiency of Fe^{2+}(as Equation (17)) [76].

Table 3 summarizes the research of domestic and foreign scholars using DBD system and Fenton oxidation process to degrade organic pollutants [77–84]. The mechanism of DBD system in collaboration with Fenton oxidation catalysis is shown in Figure 7.

Table 3. Summary of DBD technologies with Fenton oxidation for organic wastewater removal.

Researchers	Target Pollutant	Experimental Conditions	Fe^{2+} Add Quantity	Degradation Rate	Main Active Substance	Ref.
Tao et al.	MO	External applied voltage: 18.0 kV; MO concentration: 50.0 mg/L; pH: 3.0; Time: 40.0 min	120 mg/L	85.0%	·OH; H_2O_2	[77]
Reddy et al.	Methylene blue (MB)	Discharge voltage: 16.0 kV; MB concentration: 100.0 mg/L; Time: 25.0 min	60 mg/L	98.0%	·OH; HO_2·	[78]
Aziz et al.	2,4-D; 2,4-DCP	Input power: 150.0 W; 2,4-D and 2,4-DCP concentration: 100.0 mg/L; Time: 10.0 min	10 mg/L	2,4-D: 99.0%; 2,4-DCP: 95.0%	·OH	[79]
Feng et al.	Dailon	Input power: 120.0 W; Dailon concentration: 23.0 mg/L; PH: 6.2; Time: 60.0 s	30 mg/L	98.0%	·OH	[80]
Tao et al.	MO	Discharge voltage: 7.5 kV; Discharge power: 117.5 W; MO concentration: 100.0 mg/L; H_2O_2:0.6ml; Time: 13.5 min	1.0 mg/L	99.9%	·OH; h^+; $\cdot O_2^-$	[81]
Lu et al.	Orange G (OG)	Input voltage: 70.0 V; OG concentration: 100.0 mg/L; The optimum pH: 2.98; Time: 10.0 min	0.1 mmol/L	93.6%	·OH	[82]
Xu et al.	Norfloxacin (NOR)	Discharge power: 60.0 W; NOR concentration: 10.0 mg/L; Time: 15.0 min	10 mg/L	98.0%	·OH	[83]
Tao et al.	MO	MO concentration: 200.0 mg/L; Time: 6.0 min	-	99.2%	·OH; h^+; $\cdot O_2^-$	[84]

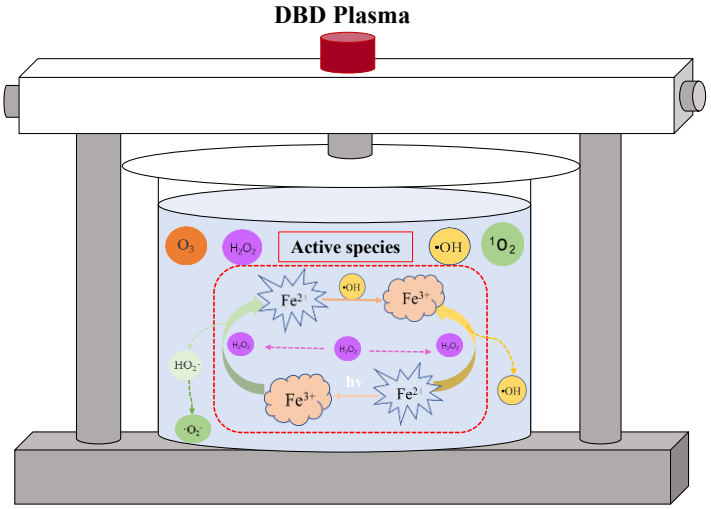

Figure 7. Mechanism of DBD coupled with a Fenton catalyst for the degradation of organic pollutants.

Feng et al. [80] added Fe^{2+} to degrade Dailon in a DBD system, and found that when Fe^{2+} was added within 10.0–30.0 mg/L, the degradation rate of Dailon increased with the increase in Fe^{2+} concentration, while the degradation rate decreased when Fe^{2+} was

added at a high concentration. In addition, the 30.0 mg/L Fe^{2+} degradation rate was 30.0% higher than 120.0 mg/L Fe^{2+}. Lu et al. [82] studied the degradation of orange G by DBD system in collaboration with Fe^{2+}. After 10.0 min of treatment under the same experimental conditions, the Fe^{2+} concentration was 0.05 mM, 0.1 mM, 0.3 mM, 0.5 mM and 0.7 mM, respectively. The corresponding degradation rates were 83.3%, 93.6%, 94.1%, 96.7% and 94.1%, respectively, while the degradation rates were only 56.7% without Fe^{2+}. These phenomena are similar to the process in Equation (15).

3.4. DBD Coupled with Persulfate Oxidation Catalysis

Persulfate (PS) oxidation is an advanced oxidation technology, which mainly relies on the strong oxidizing substance sulfate radical ($SO_4^{-}\cdot$) to degrade organic pollutants in water [85]. PS is divided into peroxymonosulfate (PMS) and peroxydisulfate (PDS) [86]. The oxidation capacity of persulfate ion ($S_2O_8^{2-}$) is not significant at room temperature, but the oxidation–reduction potential of $SO_4^{-}\cdot$ (E_0 = 2.6–3.1V) produced after activation is equivalent to ·OH (E_0 = 2.8V), which can degrade most organic pollutants in water [87,88]. The activation modes of PS mainly include light [89], electricity [90], heat [91], transition metal activation [92], etc. Their main reaction equations are shown in Equations (18)–(21) [93]:

$$S_2O_8^{2-} + hv \rightarrow 2SO_4^{-}\cdot \quad (18)$$

$$S_2O_8^{2-} + e^{-} \rightarrow SO_4^{2-} + SO_4^{-}\cdot \quad (19)$$

$$S_2O_8^{2-} + heat \rightarrow 2SO_4^{-}\cdot \quad (20)$$

$$S_2O_8^{2-} + Me^{n+} \rightarrow O_4^{-}\cdot + SO_4^{2-} + Me^{n+1} \quad (21)$$

The DBD system can produce high-energy electrons, heat and ultraviolet radiation during discharge, so it can be used to activate PS. At the same time, some reactive groups such as $\cdot O_2^{-}$ produced by the DBD system can also play the same role. The reactive free radicals $SO_4^{-}\cdot$ and ·OH generated in the process of co-catalysis oxidize the pollutants at the same time to further improve the degradation rate and energy efficiency. The specific activation principle is shown in Equations (22)–(29) [94]. $SO_4^{-}\cdot$ can be transformed into ·OH under certain conditions, and its equations are as Equations (30) and (31) [94–96].

$$S_2O_8^{2-} + plasma \rightarrow 2SO_4^{-}\cdot \quad (22)$$

$$HSO_5^{-} + plasma \rightarrow SO_4^{-}\cdot + \cdot OH \quad (23)$$

$$HOOSO_3^{-} + e^{-} \rightarrow SO_4^{2-} + \cdot OH \quad (24)$$

$$HOOSO_3^{-} + e^{-} \rightarrow SO_4^{-}\cdot + \cdot OH \quad (25)$$

$$\text{-}O_3SO\text{-}OSO_3^{-} + e^{-} \rightarrow SO_4^{-}\cdot + SO_4^{2-} \quad (26)$$

$$HOOSO_3^{-} + \cdot O_2^{-} \rightarrow SO_4^{2-} + \cdot OH^{-} + O_2 \quad (27)$$

$$HOOSO_3^{-} + \cdot O_2^{-} \rightarrow SO_4^{-}\cdot + OH^{-} + O_2 \quad (28)$$

$$\text{-}O_3SO\text{-}OSO_3^{-} + \cdot O_2^{-} \rightarrow SO_4^{-}\cdot + SO_4^{2-} + O_2 \quad (29)$$

$$\text{All pH conditions: } SO_4^{-}\cdot + H_2O \rightarrow SO_4^{2-} + \cdot OH + H^{+} \quad (30)$$

$$\text{Alkaline pH condition: } SO_4^{-}\cdot + OH^{-} \rightarrow SO_4^{2-} + \cdot OH \quad (31)$$

The mechanism diagram of DBD system cooperating with PS oxidation catalysis is shown in Figure 8. Table 4 shows the research of different scholars on the treatment of organic pollutants in water with DBD system and PS [97–104]. PS has no catalytic activity in the degradation of organic pollutants without activation. Wu et al. [99] used DBD system plasma activation potassium persulfate to degrade tetracycline (TC), and found that after 18.0 min treatment, the degradation rate of TC in the collaborative catalytic system

increased by 45.5% compared with the single DBD system. This indicates that there is a good synergistic catalytic interaction between the DBD system and PS.

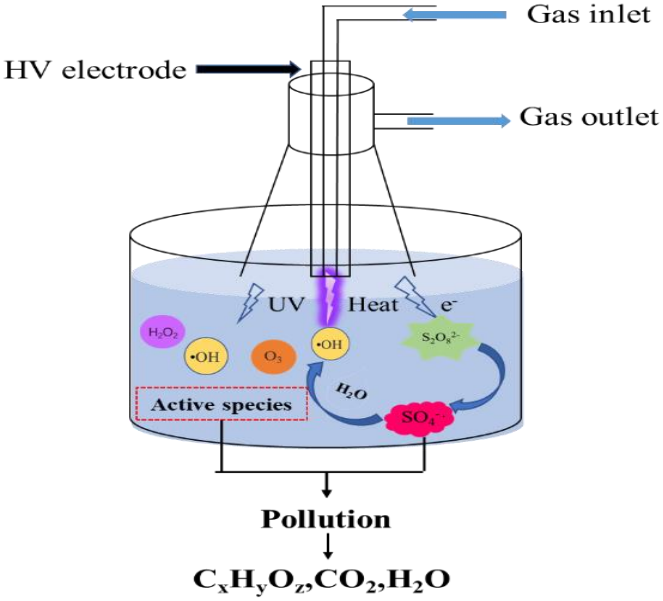

Figure 8. Mechanism of DBD coupled with PS catalyst for the degradation of organic pollutants.

Table 4. Summary of DBD technologies with persulfate oxidation for the organic wastewater removal.

Researchers	Target Pollutant	Persulfate Type	Experimental Conditions	Optimal pH	Degradation Rate	Main Active Substance	Ref.
Shang et al.	AO7	Potassium persulfate	Discharge voltage: 17.0 kV; Discharge power: 3.6 W; AO7 concentration: 5.0 mg/L; PS and AO7 add mole ratio: 100/1; Time: 50.0 min	pH = 2.6	95.0%	H_2O_2; HO_2·;·OH	[97]
Chen et al.	Acid Orange II (AO II)	Sodium persulfate	Discharge voltage: 16.0 kV; AO II concentration: 20.0 mg/L; Discharge time: 28.0 min; PS and AO II add mole ratio: 200/1	pH = 5.4	87.2%	SO_4^{-}·;·OH	[98]
Wu et al.	TC	Potassium peroxodisul-phate	Discharge voltage: 18.0 kV; TC concentration: 80.0 mg/L; PDS dosage: 120.0 mg	pH = 8.3	96.8%	SO_4^{-}·;·OH	[99]
Wang et al.	Sulfamethoxazole (SMZ)	Sodium persulfate	Discharge voltage: 180.0 V; SMX concentration: 50.0 mg/L; PS and SMX mass ratio: 40/1; Time: 30.0 min	pH = 10.3	93.4%	$·O_2^{-}$; SO_4^{-}·;·OH	[100]
Wu et al.	Benzotriazole (BTA)	Sodium persulfate	Discharge voltage: 15.0 kV; BTA concentration: 10.0 mg/L; Mass ratio of PMS and BTA: 30/1; Time: 20.0 min	pH = 3.2	97.0%	O_3;·OH	[101]
Tang et al.	TC	Potassium persulfate	Discharge voltage: 7.0 kV; TC concentration: 40.0 mg/L; PS and TC mole ratio: 20/1; Time: 15.0 min	pH = 10.0	88.2%	SO_4^{-}·;·OH	[102]
Liu et al.	Cu-EDTA	Sodium persulfate	Discharge voltage: 7.0 kV; Cu-EDTA concentration: 0.5 mmol/L; PS concentration: 2.0 mmol/L; Time: 20.0 min	pH = 5.0	100.0%	SO_4^{-}·;·OH	[103]
Wang et al.	Perfluorooctane acid (PFOA)	Potassium persulfate	Discharge voltage: 18.0 kV; PFOA concentration: 5.0 mg/L; PMS concentration: 445.0 mg/L; Time: 120.0 min	-	81.0%	SO_4^{-}·;·OH	[104]

As can be seen from Table 4, under different pH conditions, the active free radicals playing a leading role were different, and the degradation rates of various pollutants were also different. Shang et al. [97] used a DBD system in coordination with potassium persulfate to degrade TC, and the degradation rate at pH 2.6 was nearly 30.0% higher than that at pH 10.8. The reason was that acidic conditions are more conducive to the existence of $SO_4^{-}\cdot$, while alkaline conditions instead promote the transformation of $SO_4^{-}\cdot$ to ·OH.

In the DBD system co-catalyzed by PS, ·OH is the main active substance under acidic conditions, while $SO_4^{-}\cdot$ and ·OH usually play the main catalytic role under alkaline conditions. It may be attributed to the fact that some substances and phenomena produced by DBD system discharge under acidic conditions may inhibit the activity of $SO_4^{-}\cdot$. With the increase in pH, $SO_4^{-}\cdot$ in the solution gradually changes into ·OH, and with the removal of $SO_4^{-}\cdot$ activity inhibition, $SO_4^{-}\cdot$ and ·OH become the main active groups for catalytic degradation of organic pollutants when the alkalinity is not too strong. However, the mechanism of synergistic catalysis of DBD system and PS oxidation under different acid–base conditions is more complex, which requires more in-depth research.

3.5. DBD Coupled with Composite Catalysis

At present, besides the DBD system cooperating with a single catalyst, there are DBD systems which cooperate with composite catalysis, such as a DBD system cooperating with photocatalysis and adsorption, a DBD system cooperating with photocatalysis and Fenton oxidation, a DBD system cooperating with Fenton oxidation and PS oxidation, etc. Table 5 shows the research of some scholars using DBD system collaborative composite technology to treat organic pollutants in water [105–112]. It can be seen that the efficiency of the DBD system synergistic composite catalyst is higher than that of only cooperating with a single catalyst in the degradation of organic pollutants in water.

Table 5. Summary of DBD technologies with composite technology for organic wastewater removal.

Researchers	Target Pollutant	Compound Catalyst	Experimental Conditions	Degradation Rate of Composite Catalyst	Degradation Rate of Single DBD	Ref.
Wang et al.	TC	Mn/γ-Al_2O_3	Discharge power: 1.3 W; Time: 5.0 min	99.3%	69.7%	[105]
Ma et al.	Phenol	TiO_2/CeO_2	Discharge voltage: 45.0 V; Discharge power: 21.9W; Phenol concentration: 10.0 mg/L; Time: 10.0 min	97.1%	43.1%	[106]
Tang et al.	Phenol	TiO_2/GAC	Discharge voltage: 30.0 kV; Phenol concentration: 500.0 mg/L; Oxygen flow rate: 1.0 L/min; Time: 180.0 min	88.0%	-	[107]
Wang et al.	Triclocarban (TCC)	TiO_2/ACFs	Discharge power: 38.0 W; TCC concentration:10.0 mg/L; Time: 30.0 min	0.33 $mg{\cdot}L^{-1}{\cdot}min^{-1}$	0.23 $mg{\cdot}L^{-1}{\cdot}min^{-1}$	[108]
Wang et al.	Methylbenzene	$TiO_2/BaTiO_3$	Discharge power: 20.0 W; Time: 24.0 min	88.3%	59.1%	[109]
Wang et al.	MO	TiO_2/Fe_3O_4	Input voltage: 13.0 kV; TiO_2/Fe_3O_4 concentration: 100.0 mg/L; Time: 30.0 min	88.0%	-	[110]
Shang et al.	P-nitrophenol (PNP)	PS/Fe^{2+}	Discharge power: 17.0 kW; PH: 4.8–6.3; Time: 50.0 min	81.1%	34.8%	[111]
Deng et al.	Diclofenac (DCF)	Nano Fe^0/CeO_2	Discharge voltage: 12.0 kV; DCF concentration: 10.0 mg/L; PH: 7.0; Time: 10.0 min	96.4%	45.8%	[112]

As can be seen from Table 5, the DBD system often worked with photocatalysis and adsorption technology to deal with organic pollutants in water. The purpose was to solve the problem that powdered photocatalysts (such as TiO_2) were difficult to separate and recover due to agglomeration in water. In the process of DBD treatment, the combination of TiO_2 and activated carbon was not only conducive to the recycling after the end of

the experiment, but also the activated carbon could enrich the organic pollutants in the water in its pore interior or surface. At the same time, it also provided convenience for TiO_2 to treat organic pollutants and increased the degradation rate of pollutants. The DBD system could directly act on the active part of TiO_2 and activated carbon binding system to accelerate the generation of more active groups (such as ·OH and H_2O_2). In addition, the strong electric field generated by the DBD system and O_3 and H_2O_2 in solution can inhibit the electron–hole pair recombination on TiO_2, so as to improve the quantum yield of the photocatalyst. Tang et al. [107] used DBD plasma combined with TiO_2-GAC for the catalytic degradation of phenol; the degradation rate of the synergic composite catalyst increased by 20.0% compared with that of the synergic single catalyst.

The advantage of DBD plasma combined with photocatalysis and Fenton oxidation to treat organic pollutants in water is that it can make full use of UV light and H_2O_2 generated by DBD plasma. Wang et al. [110] studied the degradation of MO and found that using a DBD system in coordination with TiO_2-Fe_3O_4 had a better effect than using a single DBD system in coordination with TiO_2 and a single DBD system in coordination with Fe_3O_4, and the degradation rate of MO could reach 88.0% within 30min. Fe^{3+} could be used as an electron acceptor to capture electrons generated by TiO_2 surface excitation and reduced to produce Fe^{2+}. At the same time, the recombination of electron and hole pairs in TiO_2 photocatalyst was inhibited, and Fe^{2+} added as the electron donor made ·OH compete with the target pollutant and consumed the content of the active group ·OH in the solution. The degradation mechanism of the degradation of DCF by the DBD system-Fe_0-CeO_2 system [112] is shown in Figure 9.

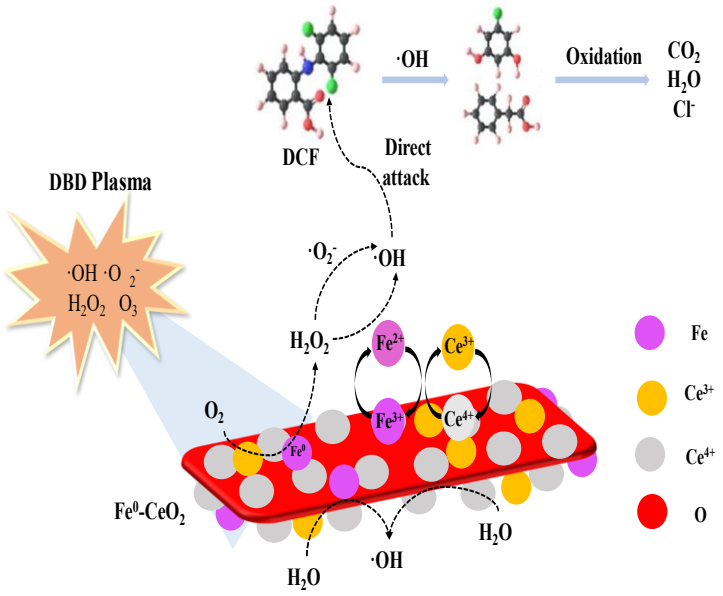

Figure 9. Mechanism of the degradation of DCF by DBD system-Fe0-CeO_2 system [112].

DBD system synergistic PS and Fenton oxidation aims to use Fe^{2+} to enhance PS activation [113]. The combined action improves the number of active groups in the solution, which can not only improve the degradation rate, but also reduce the content of Fe^{2+}, thus reducing the generation of iron sludge. Shang et al. [111] added PS-Fe^{2+} in the co-catalytic system of the DBD system and improved the degradation rate by 17.5% compared with only adding PS. Although Fenton oxidation is suitable for acidic conditions, and Fe^{2+} will produce precipitation under alkaline conditions, this experiment is more conducive to the degradation of nitrophenol under alkaline conditions. Due to the presence of O_3 and SO_4^{-}·, its reaction rate constant is larger than that of precipitation, weakening the influence of the

acid and base on Fenton oxidation and obtaining more ·OH. The specific reactions are as Equations (32)–(35) follows [111]:

$$Fe^{2+} + H_2O_2 \rightarrow Fe^{3+} + \cdot OH + OH^- \quad (32)$$

$$Fe^{2+} + S_2O_8{}^{2-} \rightarrow Fe^{3+} + SO_4{}^{-}\cdot + SO_4{}^{2-} \quad (33)$$

$$OH^- + O_3 \rightarrow O^-\cdot + \cdot OH \quad (34)$$

$$SO_4{}^{-}\cdot + OH^- \rightarrow SO_4{}^{2-} + \cdot OH \quad (35)$$

4. The Factors of DBD Coupled with Catalysis for Degradation of Wastewater

Figure 10a [64] shows the effect of manganese (Mn)-AC dosage on the degradation rate of pollutant (DMF). It can be seen that Mn-AC promoted the degradation of DMF in the DBD system, and with the increase in the dosage, the degradation of DMF first increased and then decreased. When a small amount of catalyst was added (0.5 g/L), there were insufficient catalytic active sites in the reaction system, resulting in a low DMF removal rate (71.2%). When the dosage of Mn-AC was 1.0 g/L and 1.5 g/L, the DMF removal rate increased to 82.2% and 79.4%, respectively. The results showed that more Mn-AC was involved in the reaction, thus providing more surface-active sites. Therefore, more H_2O_2 and O_3 are decomposed to form ·OH, which promotes the oxidative removal of DMF. However, too much catalyst will affect the probability of active substances' collision, resulting in a waste of resources.

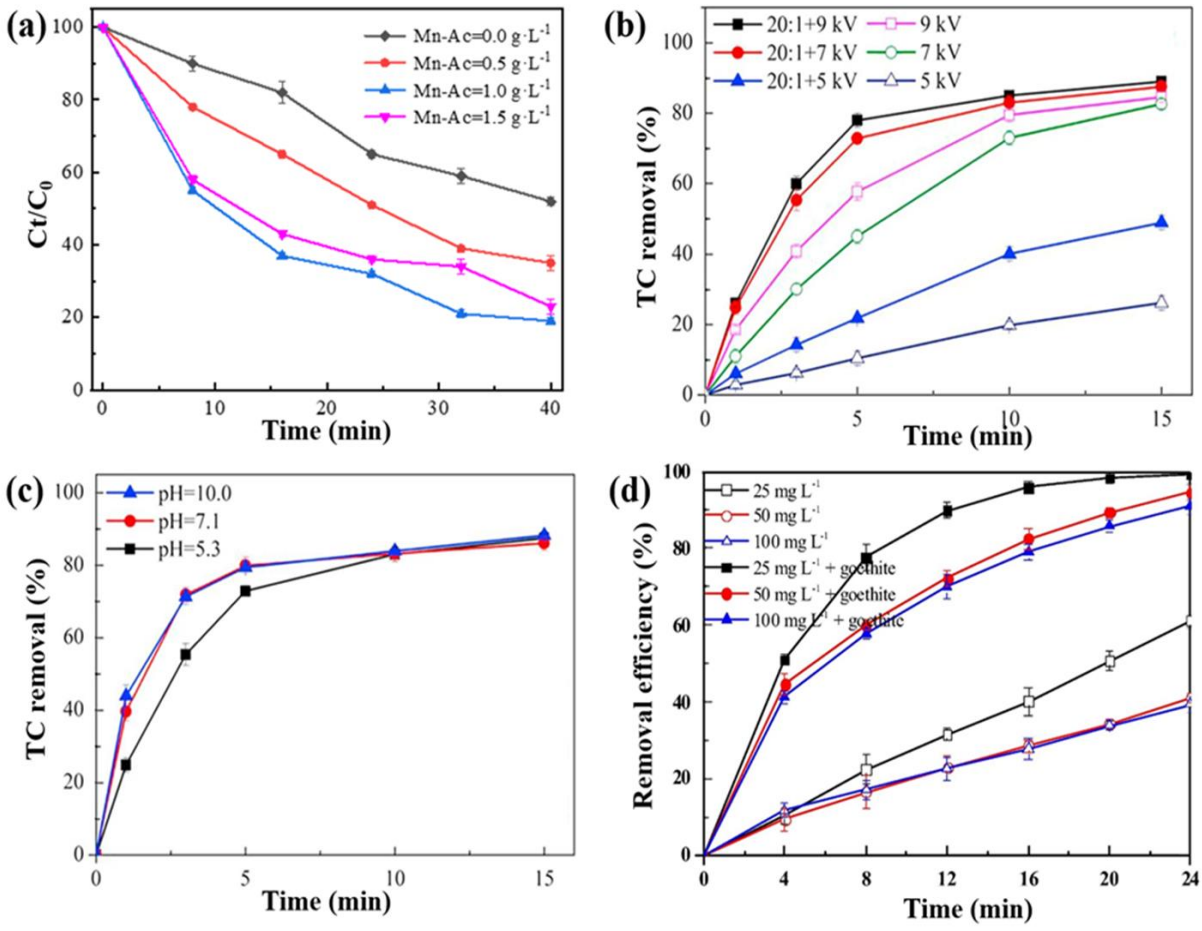

Figure 10. Effect of (**a**): catalyst dosage [64]; (**b**): peak voltage [102]; (**c**): initial pH of solution [102]; (**d**): reactant concentration [47].

Figure 10b [102] shows the influence of PS addition amount and peak voltage on TC decomposition in a DBD system. The increase in peak voltage and PS can enhance TC degradation in water. Without adding PS, the removal rate of TC was only 26.1% when DBD was treated for 15.0 min at the peak voltage of 5.0 kV, while the removal rate of TC was increased to 82.6% and 84.6% at 7.0 kV and 9.0 kV, respectively. After adding PS, the degradation rate of TC was 49.0% at the peak voltage of 5.0 kV, and increased to 87.5% and 89.0% at 7.0 kV and 9.0 kV, respectively. After the addition of PS, some physical and chemical actions (such as high-energy electrons, strong electric field, ultraviolet light, active substances, etc.) in the discharge plasma can promote the production of $\cdot SO_4^-$ by PS, and then generate more and more $\cdot SO_4^-$ and ·OH radicals. The higher the discharge voltage, the more energy is input into the reactor, and the above physicochemical interactions related to DBD plasma will be further enhanced. Water will excite more PS and form more active free radicals, thus improving the degradation rate and energy efficiency.

The effect of initial pH on TC removal is shown in Figure 10c [102]. At pH = 5.3, 7.1 and 10.0, the TC removal rates reached 87.5%, 86.1% and 88.2% after 15 min of DBD treatment, respectively. However, the degradation rate of TC in neutral and alkaline conditions was faster than that in acidic medium. Under acidic conditions, the dominant active species is O_3. As the pH increases, O_3 will rapidly decompose to ·OH. However, when the pH range is greater than 8.5, OH^- and H_2O will be oxidized by the $SO_4^-\cdot$ radical to form ·OH. Therefore, with the increase in pH value, the activation of PS and the oxidation capacity of the synergistic system can be improved simultaneously, thus promoting the degradation rate of TC. In addition, the degradation rate of TC was almost the same under neutral and alkaline conditions, indicating that the synergistic system could effectively remove TC in a wide pH range.

Figure 10d [47] shows the effect of initial concentration on the degradation rate of pollutant (caffeine). Figure 10d shows that the degradation rate of caffeine is directly related to the initial concentration. When the initial concentration of pollutants decreased from 100.0 mg/L to 25.0 mg/L, the degradation rate of caffeine in the DBD reactor alone increased from 39.0% to 61.0%, and the degradation rate of caffeine in the DBD-goethite system increased from 91.0% to 99.0%. An initial increase in caffeine concentration means that more caffeine molecules and its intermediates were present in the solution, while the number of reactive active species produced in the reaction system was constant, which led to the intensive competition of active species and a decrease in degradation rate.

5. The Process of DBD Coupled with Catalysis to Degrade Organic Pollutants

The target objects of the above studies are almost cyclic organics, and the DBD system can effectively degrade these cyclic organics. The degradation intermediates of several typical pollutants were detected by HPLC-MS [48,80,102], and their possible degradation paths are shown in Figure 11.

As can be seen from Figure 11, the hydroxylation reaction, carboxylation reaction and ring opening reaction are generally experienced in the reaction process. The active group mainly attacks C-C, C-H, C=O, C-O and O-H bonds on the organic matter and causes them to break and split into organics with smaller molecular weight. In addition, due to the existence of the carboxylation reaction, there will be organic acids in the intermediate by-products, such as oxalic acid, acetic acid, formic acid, etc. During the degradation process, pollutants are first transformed into small molecular organic matter, among which some small molecular organic matter can be decomposed into inorganic molecules and ions such as CO_2, H_2O, NH_4^+, NO_3^-, SO_4^{2-}, Cl^-, etc. However, there are still some intermediate by-products that are difficult to be degraded, resulting in the low degree of mineralization of pollutants. In the degradation of dye pollutants, the active substances produced by the DBD system first destroy the chromophore groups, such as azo bonds, and then attack the ring structure, and gradually degrade to small molecular organic matter.

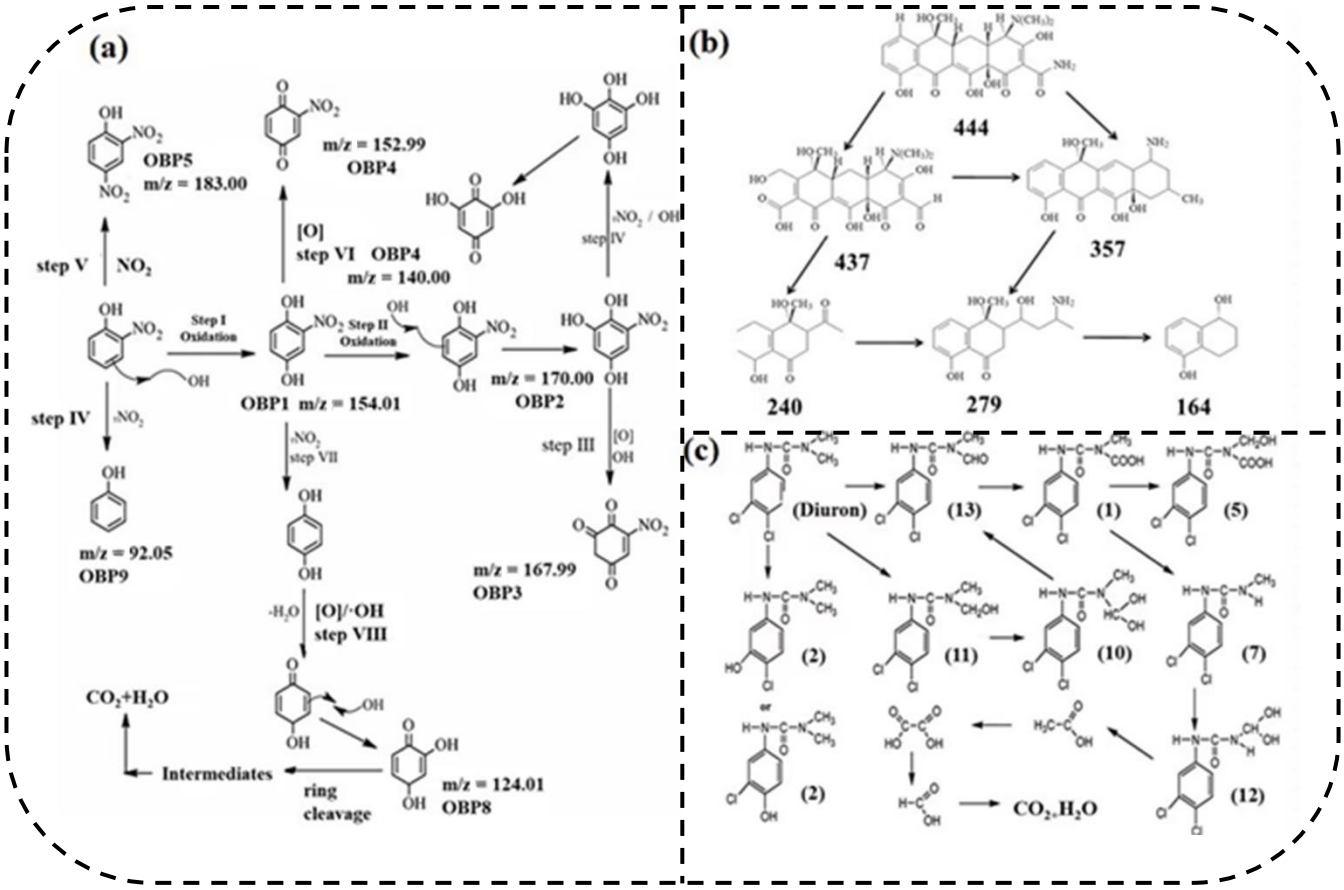

Figure 11. Degradation pathways of (**a**): 2-NP [48]; (**b**): Tetracycline [102]; (**c**): Dailon [80].

6. Energy Efficiency of DBD Coupled with Catalysis to Degrade Organic Pollutants

The energy efficiency of organic matter degradation refers to the quality of degradable organic matter per unit of energy consumption. The energy efficiency of a DBD synergistic catalytic system is higher than that of a single DBD system. Substances generated by a DBD system that cannot directly act on organic pollutants or have a poor effect on organic pollutants cannot be fully utilized. Therefore, catalysts are added in the collaborative catalytic system to make full use of these substances and convert them into free radicals that can efficiently degrade pollutants, such as ·OH, in order to enhance the degradation effect of organic pollutants in water and improve the energy efficiency.

Table 6 shows the energy efficiency of the collaborative treatment of organic pollutants in water by the DBD system adopted by some scholars [64,101–104,107,108,111,112]. Wu et al. [101] studied a DBD system in coordination with PS to degrade benzotriazole. When the input voltage increased from 11.0 kV to 13.0 kV, the energy efficiency was the highest when the input voltage was 12.0 kV, which could reach 1.5–1.8 g/kWh, and its energy efficiency was higher than that of a single DBD system. Wang et al. [109] carried out an experiment of a DBD system in coordination with a TiO_2-$BaTiO_3$ catalytic system to degrade toluene. With the increase in input power, its energy also output first reached the maximum value and then decreased.

Table 6. Energy efficiency of DBD technologies for organic wastewater removal in different systems.

Researchers	Target Pollutant	Catalyst	Initial Concentration	Degradation Rate	Energy Efficiency of Single DBD System	Energy Efficiency of Co-Catalysis	Ref.
Sang et al.	DMF	Mn-AC	1000.0 mg/L	82.2%	-	74,844.0 mg/kWh	[64]
Wu et al.	BTA	Sodium persulfate	10.0 mg/L	97.0%	910.0 mg/kWh	1670.0 mg/kWh	[101]
Tang et al.	TC	Potassium persulfate	40.0 mg/L	49.0%	23.7 mg/kJ	160,200.0 mg/kWh	[102]
Wang et al.	PFOA	Potassium persulfate/O_3	5.0 mg/L	94.8%	72.5 mg/kWh	120.0 mg/kWh	[103]
Wang et al.	TC	Mn/γ/Al_2O_3	-	99.3%	-	91,700.0 mg/kWh	[104]
Tang et al.	Phenol	TiO_2/GAC	500.0 mg/L	88.0%	-	GAC:5760.0 mg/kWh; TiO_2-GAC:6840.0 mg/kWh	[107]
Wang et al.	TCC	TiO_2/ACFs	10.0 mg/L	84.9%	30.0 mg/kWh	45.0 mg/kWh	[108]
Shang et al.	PNP	PS/Fe^{2+}	5.0 mg/L	81.1%	-	Fe^{2+}:200.0 mg/kWh; PS:180.0 mg/kWh; PS-Fe^{2+}:230.0 mg/kWh	[111]
Deng et al.	DCF	Nano Fe^0/CeO_2	10.0 mg/L	96.4%	2460.0 mg/kWh	Fe^0:5350.0 mg/kWh; Fe^0 -CeO_2:9940.0 mg/kWh	[112]

The energy efficiency of a DBD system is mainly affected by input power and voltage. With the increase in input power and voltage in a certain range, its energy efficiency will also increase. This is because the increase in input power and input voltage will lead to the increase in active substances in the DBD system's cooperative catalytic system and the strengthening of the effect of physical phenomena [23]. For example, the increase in ultraviolet radiation intensity will enhance the energy efficiency of DBD system's cooperative photocatalytic system and the enhancement of the thermal effect will make PS more easily activated. However, when the input power and input voltage continue to increase beyond a certain range, local spark discharge will occur, making the DBD system discharge uneven. In addition, excessive energy input will convert part of electric energy into heat, resulting in an increase in the temperature of the system and the decomposition of ozone in the solution, thus reducing the degradation efficiency and reducing the energy efficiency [101,109].

7. Summary and Prospect

DBD is widely used to deal with the degradation of organic pollutants, and the addition of a catalyst can improve the output of active substances, thereby improving the plasma energy utilization and organic-matter removal efficiency. However, as time goes on, the following problems still need to be studied in depth.

(1) The mechanism of DBD plasma activating the catalyst is relatively complex. How to use advanced means to understand the catalytic mechanism and catalytic reaction process is the first problem to be clarified in the future.
(2) The effect of catalyst addition on the degradation process of organic compounds was rarely reported in the past literature, which needs further exploration.
(3) DBD plasma can affect the catalyst to a certain extent. Therefore, it is imperative to study how to reduce or avoid the damage caused by DBD plasma to the catalyst.
(4) The separation and recovery of catalysts are generally difficult. It not only consumes a large amount of catalyst to increase the treatment cost, but also causes secondary pollution to the environment. The subsequent goal is to study how to recover and reuse the catalyst in DBD plasma.
(5) At present, there are few toxicity analyses related to the degradation of organic pollutants by DBD plasma coupled with catalysts. It is uncertain whether more toxic substances were produced during the degradation process. Therefore, some methods should be used to characterize the toxicity changes in the process of pollutant degradation.
(6) The research on the degradation of organic pollutants by DBD plasma coupled with catalysts are still in the laboratory stage. How to expand the reactor scale and realize the industrial application of DBD plasma synergetic catalysis are urgent problems to be solved.

Author Contributions: H.G.: writing—original draft preparation; data curation. Y.S. writing—original draft preparation; investigation; X.Y. Conceptualization, methodology; investigation. Y.W. (Yawen Wang)**:** investigation. Z.L.: methodology; investigation. Y.W. (Yifeng Wu): supervision, project administration; J.R.: Writing—review and editing, investigation and visualization. All authors have read and agreed to the published version of the manuscript.

Funding: We greatly appreciate financial support from National Natural Science Foundation of China (No. 22006069), Natural Science Foundation of Jiangsu Province in China, (No. BK20200801), Natural Science Foundation of the Jiangsu Higher Education Institution of China (No. 20KJB610015), Postdoctoral Science Foundation of Jiangsu Province in China (No. 2021K592C), and Postgraduate Research & Practice Innovation Program of Jiangsu Province (No. SJCX22_0322; SJCX21_0343).

Conflicts of Interest: The authors declare no conflict of interest.

References

1. El-Nahhal, I.; El-Nahhal, Y. Pesticide residues in drinking water, their potential risk to human health and removal options. *J. Environ. Manag.* **2021**, *299*, 113611. [CrossRef] [PubMed]
2. Panigrahy, N.; Priyadarshini, A.; Sahoo, M.M.; Verma, A.K.; Daverey, A.; Sahoo, N.K. A comprehensive review on eco-toxicity and biodegradation of phenolics: Recent progress and future outlook. *Environ. Technol. Innov.* **2022**, *27*, 102423. [CrossRef]
3. Qiao, M.; Ying, G.G.; Singer, A.C.; Zhu, Y.G. Review of antibiotic resistance in China and its environment. *Environ. Int.* **2018**, *110*, 160–172. [CrossRef] [PubMed]
4. Rania, A.T.; Ali, S.S.; Li, F.; Okasha, K.M.; Mahmoud, Y.A.G.; Elsamahy, T.; Jiao, H.X.; Fu, Y.Y.; Sun, J.Z. A critical review on the treatment of dye-containing wastewater: Ecotoxicological and health concerns of textile dyes and possible remediation approaches for environmental safety. *Ecotoxicol. Environ. Saf.* **2022**, *231*, 113160.
5. Khan, M.A.; Wabaidur, S.M.; Siddiqui, M.R.; Alqadami, A.A.; Khan, A.H. Silico-manganese fumes waste encapsulated cryogenic alginate beads for aqueous environment de-colorization. *J. Clean. Prod.* **2020**, *244*, 118867. [CrossRef]
6. Kumar, J.A.; Krithiga, T.; Sathish, S.; Renita, A.A.; Prabu, D.; Lokesh, S.; Geetha, R.; Namasivayam, S.K.R.; Sillanpaa, M. Persistent organic pollutants in water resources: Fate, occurrence, characterization and risk analysis. *Sci. Total Environ.* **2022**, *831*, 154808. [CrossRef]
7. Katheresan, V.; Kansedo, J.; Lau, S.Y. Efficiency of various recent wastewater dye removal methods: A review. *J. Environ. Chem. Eng.* **2018**, *6*, 4676–4697. [CrossRef]
8. Alexandre, G.; Moura, B.A. Membrane Separation Process in Wastewater and Water Purification. *Membranes* **2022**, *12*, 259.
9. Wang, Y.; Jin, X.; Yang, S.; Wang, G.; Xu, L.; Jin, P.; Shi, X.; Shi, Y. Interactions between flocs and bubbles in the separation zone of dissolved air flotation system. *Sci. Total Environ.* **2022**, *761*, 143222. [CrossRef]
10. Rashid, R.; Shafiq, I.; Akhter, P.; Iqbal, M.J.; Hussain, M. A state-of-the-art review on wastewater treatment techniques: The effectiveness of adsorption method. *Environ. Sci. Pollut. Res.* **2021**, *28*, 9050–9066. [CrossRef]
11. Azam, M.; Wabaidur, S.M.; Khan, M.R.; Al-Resayes, S.I.; Islam, M.S. Heavy metal ions removal from aqueous solutions by treated ajwa date pits: Kinetic, isotherm, and thermodynamic approach. *Polymers* **2022**, *14*, 914. [CrossRef] [PubMed]
12. Saravanan, A.; Kumar, P.S.; Jeevanantham, S.; Karishma, S.; Tajsabreen, B.; Yaashikaa, P.R.; Reshma, B. Effective water/wastewater treatment methodologies for toxic pollutants removal: Processes and applications towards sustainable development. *Chemosphere* **2021**, *280*, 130595. [CrossRef]
13. Abujazar, M.S.S.; Karaağaç, S.U.; Abu Amr, S.S.; Alazaiza, M.Y.D.; Bashir, M.J.K. Recent advancement in the application of hybrid coagulants in coagulation-flocculation of wastewater: A review. *J. Clean. Prod.* **2022**, *345*, 131133. [CrossRef]
14. Mohammadi, S.A.; Najafi, H.; Zolgharnian, S.; Sharifian, S.; Asasian-Kolur, N. Biological oxidation methods for the removal of organic and inorganic contaminants from wastewater: A comprehensive review. *Sci. Total Environ.* **2022**, *843*, 157026. [CrossRef] [PubMed]
15. Priyadarshini, M.; Das, I.; Ghangrekar, M.M.; Blaney, L. Advanced oxidation processes: Performance, advantages, and scale-up of emerging technologies. *J. Environ. Manag.* **2022**, *316*, 115295. [CrossRef] [PubMed]
16. Ziembowicz, S.; Kida, M. Limitations and future directions of application of the Fenton-like process in micropollutants degradation in water and wastewater treatment: A critical review. *Chemosphere* **2022**, *296*, 134041. [CrossRef] [PubMed]
17. Lim, S.; Shi, J.L.; Gunten, U.; McCurry, D.L. Ozonation of organic compounds in water and wastewater: A critical review. *Water Res.* **2022**, *213*, 118053.
18. Saeed, M.; Muneer, M.; Haq, A.U.; Akram, N. Photocatalysis: An effective tool for photodegradation of dyes—A review. *Environ. Sci. Pollut. Res.* **2022**, *29*, 293–311. [CrossRef]
19. Qiao, J.; Xiong, Y.Z. Electrochemical oxidation technology: A review of its application in high-efficiency treatment of wastewater containing persistent organic pollutants. *J. Water Process Eng.* **2021**, *44*, 102308. [CrossRef]
20. Eren, Z. Ultrasound as a basic and auxiliary process for dye remediation: A review. *J. Environ. Manag.* **2012**, *104*, 127–141. [CrossRef]
21. Wang, B.W.; Wang, Y. A comprehensive review on persulfate activation treatment of wastewater. *Sci. Total Environ.* **2022**, *831*, 154906. [CrossRef] [PubMed]

22. Ma, S.; Kim, K.; Chun, S.; Moon, S.Y.; Hong, Y. Plasma-assisted advanced oxidation process by a multi-hole dielectric barrier discharge in water and its application to wastewater treatment. *Chemosphere* **2020**, *243*, 125377. [CrossRef] [PubMed]
23. Guo, H.; Wang, Y.; Liao, L.; Li, Z.; Pan, S.; Puyang, C.; Su, Y.; Zhang, Y.; Wang, T.; Ren, J.; et al. Review on remediation of organic-contaminated soil by discharge plasma: Plasma types, impact factors, plasma-assisted catalysis, and indexes for remediation. *Chem. Eng. J.* **2022**, *436*, 135239. [CrossRef]
24. Yang, J.R.; Zeng, D.Q.; Muhammad, H.; Ma, Z.B.; Dong, L.Q.; Xie, Y.; He, Y.L. Efficient degradation of Bisphenol A by dielectric barrier discharge non-thermal plasma: Performance, degradation pathways and mechanistic consideration. *Chemosphere* **2022**, *286*, 131627. [CrossRef]
25. Piskarev, I.M. Corona Electric Discharge as a Source of Chemically Active Species. *Plasma Chem. Plasma Process.* **2021**, *41*, 1415–1434. [CrossRef]
26. Du, C.M.; Yan, J.H.; Cheron, B.G. Degradation of 4-chlorophenol using a gas-liquid gliding arc discharge plasma reactor. *Plasma Chem. Plasma Process.* **2007**, *27*, 635–646. [CrossRef]
27. Wang, X.Y.; Zhou, M.H.; Jin, X.L. Application of glow discharge plasma for wastewater treatment. *Electrochim. Acta* **2012**, *83*, 501–512. [CrossRef]
28. Bilea, F.; Bradu, C.; Mandache, N.B.; Magureanu, M. Characterization of the chemical activity of a pulsed corona discharge above water. *Chemosphere* **2019**, *236*, 124302. [CrossRef]
29. Magureanu, M.; Bilea, F.; Bradu, C.; Hong, D. A review on non-thermal plasma treatment of water contaminated with antibiotics. *J. Hazard. Mater.* **2021**, *417*, 125481. [CrossRef]
30. Massima, M.E.S.; Tijani, J.O.; Badmus, K.O.; Pereao, O.; Babajide, O.; Fatoba, O.O.; Zhang, C.; Shao, T.; Sosnin, E.; Tarasenko, V.; et al. A critical review on ozone and co-species, generation and reaction mechanisms in plasma induced by dielectric barrier discharge technologies for wastewater remediation. *J. Environ. Chem. Eng.* **2021**, *9*, 105758.
31. Shang, K.F.; Li, J.; Morent, R. Hybrid electric discharge plasma technologies for water decontamination-a short review. *Plasma Sci. Technol.* **2019**, *21*, 5–13. [CrossRef]
32. Liang, J.P.; Zhou, X.F.; Zhao, Z.L.; Yang, D.Z.; Wang, W.C.; Addou, A. Degradation of trimethoprim in aqueous by persulfate activated with nanosecond pulsed gas-liquid discharge plasma. *J. Environ. Manag.* **2021**, *278*, 111539. [CrossRef] [PubMed]
33. Wang, T.C.; Jia, H.Z.; Guo, X.T.; Xia, T.J.; Qu, G.Z.; Sun, Q.H.; Yin, X.Q. Evaluation of the potential of dimethyl phthalate degradation in aqueous using sodium percarbonate activated by discharge plasma. *Chem. Eng. J.* **2018**, *346*, 65–76. [CrossRef]
34. Ren, J.Y.; Jiang, N.; Shang, K.F.; Lu, N.; Li, J.; Wu, Y. Synergistic degradation of trans-ferulic acid by water falling film DBD plasma coupled with cobalt oxyhydroxide: Performance and mechanisms. *Chem. Eng. J.* **2019**, *372*, 321–331. [CrossRef]
35. Fang, C.; Wang, S.H.; Shao, C.S.; Liu, C.; Wu, Y.H.; Huang, Q. Study of detoxification of methyl parathion by dielectric barrier discharge (DBD) non-thermal plasma at gas-liquid interface: Mechanism and bio-toxicity evaluation. *Chemosphere* **2022**, *307*, 135620. [CrossRef]
36. Ren, J.Y.; Song, H.Z.; Guo, H.; Yao, Z.Z.; Wei, Q.; Jiao, K.Q.; Li, Z.Y.; Zhong, C.C.; Wang, J.; Zhen, Y.Z. Removal of chloramphenicol in water by an improved water falling film dielectric barrier discharge reactor: Performance, mechanism, degradation pathway and toxicity evaluation. *J. Clean. Prod.* **2021**, *325*, 129332. [CrossRef]
37. Hu, X.Y.; Wang, B.W. Removal of pefloxacin from wastewater by dielectric barrier discharge plasma: Mechanism and degradation pathways. *J. Environ. Chem. Eng.* **2021**, *9*, 105720. [CrossRef]
38. Kim, K.S.; Kam, S.K.; Mok, Y.S. Elucidation of the degradation pathways of sulfonamide antibiotics in a dielectric barrier discharge plasma system. *Chem. Eng. J.* **2015**, *271*, 31–42. [CrossRef]
39. Sahu, D. Degradation of Industrial Phenolic Wastewater Using Dielectric Barrier Discharge Plasma Technique. *Russ. J. Appl. Chem.* **2022**, *93*, 905–915. [CrossRef]
40. Fan, J.W.; Wu, H.X.; Liu, R.Y.; Meng, L.Y.; Sun, Y.J. Review on the treatment of organic wastewater by discharge plasma combined with oxidants and catalysts. *Environ. Sci. Pollut. Res.* **2021**, *28*, 2522–2548. [CrossRef]
41. Hafeez, A.; Shezad, N.; Javed, F.; Fazal, T.; Rehman, M.S.; Rehman, F. Synergetic effect of packed-bed corona-DBD plasma micro-reactor and photocatalysis for organic pollutant degradation. *Sep. Purif. Technol.* **2021**, *269*, 118728. [CrossRef]
42. Qi, K.Z.; Cheng, B.; Yu, J.G.; Ho, W.K. A review on TiO_2-based Z-scheme photocatalysts. *Chin. J. Catal.* **2017**, *38*, 1936–1955. [CrossRef]
43. Shayegan, Z.; Lee, C.S.; Haghighat, F. TiO_2 photocatalyst for removal of volatile organic compounds in gas phase—A review. *Chem. Eng. J.* **2018**, *334*, 2408–2439. [CrossRef]
44. Chen, D.J.; Cheng, Y.L.; Zhou, N.; Chen, P.; Wang, Y.P.; Li, K.; Huo, S.H.; Cheng, P.F.; Peng, P.; Zhang, R.C.; et al. Photocatalytic degradation of organic pollutants using TiO_2-based photocatalysts: A review. *J. Clean. Prod.* **2020**, *268*, 121725. [CrossRef]
45. Mena, E.; Rey, A.; Beltrán, F.J. TiO_2 photocatalytic oxidation of a mixture of emerging contaminants: A kinetic study independent of radiation absorption based on the direct-indirect model. *Chem. Eng. J.* **2018**, *339*, 369–380. [CrossRef]
46. Wang, J.; Sun, Y.B.; Jiang, H.; Feng, J.W. Removal of caffeine from water by combining dielectric barrier discharge (DBD) plasma with goethite. *J. Saud. Chem. Soc.* **2016**, *21*, 545–557. [CrossRef]
47. Hu, X.; Hu, X.J.; Peng, Q.Q.; Zhou, L.; Tan, X.F.; Jiang, L.H.; Tang, C.F.; Wang, H.; Liu, S.H.; Wang, Y.Q.; et al. Mechanisms underlying the photocatalytic degradation pathway of ciprofloxacin with heterogeneous TiO_2. *Chem. Eng. J.* **2020**, *380*, 122366. [CrossRef]
48. Tijani, J.O.; Mouele, M.E.S.; Tottito, T.C.; Fatoba, O.O.; Petrik, L.F. Degradation of 2-nitrophenol by dielectric barrier discharge system: The influence of carbon doped TiO_2 photocatalyst supported on stainless steel mesh. *Plasma Chem. Plasma Process.* **2017**, *37*, 1343–1373. [CrossRef]

49. Li, S.P.; Ma, X.L.; Liu, L.J.; Cao, X.H. Degradation of 2,4-dichlorophenol in wastewater by low temperature plasma coupled with TiO_2 photocatalysis. *RSC Adv.* **2015**, *5*, 1902–1909. [CrossRef]
50. Li, S.P.; Chen, H.; Wang, X.P.; Dong, X.C.; Huang, Y.X.; Guo, D. Catalytic degradation of clothianidin with graphene/TiO_2 using a dielectric barrier discharge (DBD) plasma system. *Environ. Sci. Pollut. Res.* **2020**, *27*, 29599–29611. [CrossRef]
51. Tao, X.M.; Yang, C.; Huang, L.; Shang, S.Y. Novel plasma assisted preparation of ZnCuFeCr layered double hydroxides with improved photocatalytic performance of methyl orange degradation. *Appl. Surf. Sci.* **2020**, *507*, 145053. [CrossRef]
52. Wang, H.J.; Shen, Z.; Yan, X.; Guo, H.; Mao, D.N.; Yi, C.W. Dielectric barrier discharge plasma coupled with WO_3 for bisphenol A degradation. *Chemosphere* **2021**, *274*, 129722. [CrossRef]
53. Tao, X.M.; Han, Y.Y.; Sun, C.; Huang, L.; Xu, D.Y. Plasma modification of NiAlCe–LDH as improved photocatalyst for organic dye wastewater degradation. *Appl. Clay Sci.* **2019**, *172*, 75–79. [CrossRef]
54. Liu, X.W.; Li, W.Q.; Hu, R.; Wei, Y.; Yun, W.Y.; Nian, P.; Feng, J.W.; Zhang, A.Y. Synergistic degradation of acid orange 7 dye by using non-thermal plasma and g-C_3N_4/TiO_2: Performance, degradation pathways and catalytic mechanism. *Chemosphere* **2020**, *249*, 126093. [CrossRef]
55. Rathi, B.S.; Kumar, P.S. Application of adsorption process for effective removal of emerging contaminants from water and wastewater. *Environ. Pollut.* **2021**, *280*, 116995. [CrossRef]
56. Islam, M.; Hossain, M.; Mahbub, S.; Hoque, M.A.; Kumar, D.; Wabaidur, S.M.; Habila, M.A.; AL-Anazy, M.M.; Kabir, M. Influences of alcohol and diol on the aggregation behaviour, modes of interaction and the thermodynamic properties of the mixture of bromocresol green dye and sodium dodecyl sulphate at numerous temperatures. *Mol. Phys.* **2021**, *119*, e1925364. [CrossRef]
57. Liu, Z.; Mohseni, M.; Sauvé, S.; Barbeau, B. Segmented regeneration of ion exchange resins used for natural organic matter removal. *Sep. Purif. Technol.* **2022**, *303*, 122271. [CrossRef]
58. Bhadra, B.N.; Seo, P.W.; Jhung, S.H. Adsorption of diclofenac sodium from water using oxidized activated carbon. *Chem. Eng. J.* **2016**, *301*, 27–34. [CrossRef]
59. Jiang, N.; Shang, R.; Heijman, S.G.J.; Rietveld, L.C. High-silica zeolites for adsorption of organic micro-pollutants in water treatment: A review. *Water Res.* **2018**, *144*, 145–161. [CrossRef]
60. Srivastava, A.; Gupta, B.; Majumder, A.; Gupta, A.K.; Nimbhorkar, S.K. A comprehensive review on the synthesis, performance, modifications, and regeneration of activated carbon for the adsorptive removal of various water pollutants. *J. Environ. Chem. Eng.* **2021**, *9*, 106177. [CrossRef]
61. Latip, N.M.B.; Gopal, K.; Suwaibatu, M.; Hashim, N.M.; Rahim, N.Y.; Raoov, M.; Yahaya, N.; Zain, N.N.M. Removal of 2,4-dichlorophenol from wastewater by an efficient adsorbent of magnetic activated carbon. *Sep. Sci. Technol.* **2021**, *56*, 252–265. [CrossRef]
62. Tang, S.F.; Li, N.; Qi, J.B.; Yuan, D.L.; Li, J. Degradation of phenol using a combination of granular activated carbon adsorption and bipolar pulse dielectric barrier discharge plasma regeneration. *Plasma Sci. Technol.* **2018**, *20*, 054013. [CrossRef]
63. Gushchin, A.A.; Gusev, G.I.; Grinevich, V.I.; Izvekova, T.V.; Kvitkova, E.Y.; Rybkin, V.V. Destruction of 2,4-Dichlorophenol in water solution using a combined process of sorption and plasma exposure to DBD. *Plasma Chem. Plasma Process.* **2021**, *41*, 421–431. [CrossRef]
64. Sang, W.J.; Mei, L.J.; Zhan, C.; Zhang, Q.; Jin, X.; Zhang, S.H.; Zhang, S.Y.; Li, C.H.; Li, M. Removal of N, N-dimethylformamide by dielectric barrier discharge plasma combine with manganese activated carbon. *Environ. Sci. Pollut. Res. Int.* **2021**, *28*, 41698–41711. [CrossRef]
65. Gong, S.; Sun, Y.B.; Zheng, K.; Jiang, G.L.; Li, L.; Feng, J.W. Degradation of levofloxacin in aqueous solution by non-thermal plasma combined with Ag_3PO_4/activated carbon fibers: Mechanism and degradation pathways. *Sep. Purif. Technol.* **2020**, *250*, 117264. [CrossRef]
66. Lu, N.; Li, J.; Wang, X.X.; Wang, T.C.; Wu, Y. Application of double-dielectric barrier discharge plasma for removal of pentachlorophenol from wastewater coupling with activated carbon adsorption and simultaneous regeneration. *Plasma Chem. Plasma Process.* **2012**, *32*, 109–121. [CrossRef]
67. Qu, G.Z.; Lu, N.; Li, J.; Wu, Y.; Li, G.F.; Li, D. Simulataneous pentachlorophenol decomposition and granular activated carbon regeneration assisted by dielectric barrier discharge plasma. *J. Hazard. Mater.* **2009**, *172*, 472–478. [CrossRef]
68. Tang, S.F.; Lu, N.; Li, J.; Wu, Y. Design and application of an up-scaled dielectric barrier discharge plasma reactor for regeneration of phenol-saturated granular activated carbon. *Sep. Purif. Technol.* **2012**, *95*, 73–79. [CrossRef]
69. Thomas, N.; Dionysiou, D.D.; Pillai, S.C. Heterogeneous Fenton catalysts: A review of recent advances. *J. Hazard. Mater.* **2021**, *404*, 124082. [CrossRef]
70. Furia, F.; Minella, M.; Gosetti, F.; Turci, F.; Sabatino, R.; Cesare, A.D.; Corno, G.; Vione, D. Elimination from wastewater of antibiotics reserved for hospital settings, with a Fenton process based on zero-valent iron. *Chemosphere* **2021**, *283*, 131170. [CrossRef]
71. Ribeiro, J.P.; Nunes, M.I. Recent trends and developments in Fenton processes for industrial wastewater treatment—A critical review. *Environ. Res.* **2021**, *197*, 110957. [CrossRef] [PubMed]
72. Liu, X.C.; Zhou, Y.Y.; Zhang, J.C.; Luo, L.; Yang, Y.; Huang, H.L.; Peng, H.; Tang, L.; Mu, Y. Insight into electro-Fenton and photo-Fenton for the degradation of antibiotics: Mechanism study and research gaps. *Chem. Eng. J.* **2018**, *347*, 379–397. [CrossRef]
73. Moratalla, Á.; Araújo, D.M.; Moura, G.O.M.A.; Lacasa, E.; Cañizares, P.; Rodrigo, M.A.; Sáez, C. Pressurized electro-Fenton for the reduction of the environmental impact of antibiotics. *Sep. Purif. Technol.* **2021**, *276*, 119398. [CrossRef]

74. Kodavatiganti, S.; Bhat, A.P.; Gogate, P.R. Intensified degradation of Acid Violet 7 dye using ultrasound combined with hydrogen peroxide, Fenton, and persulfate. *Sep. Purif. Technol.* **2021**, *279*, 119673. [CrossRef]
75. Zhang, Q.; Li, Y.; Li, H.; Zhang, Y.H.; Zhang, L.S.; Zhong, S.; Shu, X.H. Multi-catalysis of glow discharge plasma coupled with FeS_2 for synergistic removal of antibiotic. *Chemosphere* **2023**, *312*, 137204. [CrossRef]
76. Ramos, M.D.N.; Santana, C.S.; Velloso, C.C.V.; Silva, A.H.M.; Magalhães, F.; Aguiar, A. A review on the treatment of textile industry effluents through Fenton processes. *Process Saf. Environ. Prot.* **2021**, *155*, 366–386. [CrossRef]
77. Tao, X.M.; Sun, C.; Huang, L.; Han, Y.Y.; Xu, D.Y. Fe-MOFs prepared with the DBD plasma method for efficient Fenton catalysis. *RSC Adv.* **2019**, *9*, 6379–6386. [CrossRef]
78. Reddy, P.M.K.; Raju, B.R.; Karuppiah, J.; Reddy, E.L.; Subrahmanyam, C. Degradation and mineralization of methylene blue by dielectric barrier discharge non-thermal plasma reactor. *Chem. Eng. J.* **2013**, *217*, 41–47. [CrossRef]
79. Aziz, K.H.H.; Miessner, H.; Mueller, S.; Mahyar, A.; Kalass, D.; Moeller, D.; Khorshid, I.; Rashid, M.A.M. Comparative study on 2,4-dichlorophenoxyacetic acid and 2,4-dichlorophenol removal from aqueous solutions via ozonation, photocatalysis and non-thermal plasma using a planar falling film reactor. *J. Hazard. Mater.* **2018**, *343*, 107–115. [CrossRef]
80. Feng, J.W.; Zheng, Z.; Sun, Y.B.; Luan, J.F.; Wang, Z.; Wang, L.H.; Feng, J.F. Degradation of diuron in aqueous solution by dielectric barrier discharge. *J. Hazard. Mater.* **2008**, *154*, 1081–1089. [CrossRef]
81. Tao, X.M.; Yang, C.; Wei, Z.H.; Huang, L.; Chen, J.X.; Cong, W.W.; Xie, R.Y.; Xu, D.Y. Synergy between Fenton process and DBD for methyl orange degradation. *Mater. Res. Bull.* **2019**, *120*, 110581. [CrossRef]
82. Lu, W.; Sang, W.J.; Jia, D.N.; Zhang, Q.; Li, C.H.; Zhang, S.Y.; Zhan, C.; Mei, L.J.; Li, M. Improvement of degradation of Orange G in aqueous solution by Fe^{2+} added in dielectric barrier discharge plasma system. *J. Water Process Eng.* **2022**, *47*, 102707. [CrossRef]
83. Xu, Z.M.; Xue, X.J.; Hu, S.H.; Li, Y.X.; Shen, J.; Lan, Y.; Zhou, R.X.; Yang, F.; Cheng, C. Degradation effect and mechanism of gas-liquid phase dielectric barrier discharge on norfloxacin combined with H_2O_2 or Fe^{2+}. Sep. *Purif. Technol.* **2020**, *230*, 115862. [CrossRef]
84. Tao, X.M.; Yuan, X.J.; Huang, L. Effects of Fe (II)/Fe (III) of Fe-MOFs on catalytic performance in plasma/Fenton-like system. *Colloids Surf. A* **2021**, *610*, 125745. [CrossRef]
85. Lee, J.; Gunten, U.; Kim, J.H. Persulfate-based advanced oxidation: Critical assessment of opportunities and roadblocks. *Environ. Sci. Technol.* **2020**, *54*, 3064–3081. [CrossRef]
86. Ghanbari, F.; Moradi, M. Application of peroxymonosulfate and its activation methods for degradation of environmental organic pollutants: Review. *Chem. Eng. J.* **2017**, *310*, 41–62. [CrossRef]
87. Ike, I.A.; Linden, K.G.; Orbell, J.D.; Duke, M. Critical review of the science and sustainability of persulphate advanced oxidation processes. *Chem. Eng. J.* **2018**, *338*, 651–669. [CrossRef]
88. Wacławek, S.; Lutze, H.V.; Grübel, K.; Padil, V.V.T.; Černík, M.; Dionysiou, D.D. Chemistry of persulfates in water and wastewater treatment: A review. *Chem. Eng. J.* **2017**, *330*, 44–62. [CrossRef]
89. Ye, J.S.; Zhou, P.L.; Chen, Y.; Ou, H.; Liu, J.; Li, C.S.; Li, Q.S. Degradation of 1H-benzotriazole using ultraviolet activating persulfate: Mechanisms, products and toxicological analysis. *Chem. Eng. J.* **2018**, *334*, 1493–1501. [CrossRef]
90. Matzek, L.W.; Tipton, M.J.; Farmer, A.T.; Steen, A.D.; Carter, K.E. Understanding electrochemically activated persulfate and its application to ciprofloxacin abatement. *Environ. Sci. Technol.* **2018**, *52*, 5875–5883. [CrossRef]
91. Manz, K.E.; Carter, K.E. Investigating the effects of heat activated persulfate on the degradation of furfural, a component of hydraulic fracturing fluid chemical additives. *Chem. Eng. J.* **2017**, *327*, 1021–1032. [CrossRef]
92. Qiu, Q.L.L.; Li, G.X.; Dai, Y.; Xu, Y.Y.; Bao, P. Removal of antibiotic resistant microbes by Fe (II)-activated persulfate oxidation. *J. Hazard. Mater.* **2020**, *396*, 122733. [CrossRef]
93. Zou, L.X.; Wang, Y.; Huang, C.; Li, B.B.; Lyu, J.; Wang, S.; Lu, H.; Li, J. Meta-cresol degradation by persulfate through UV/O_3 synergistic activation: Contribution of free radicals and degradation pathway. *Sci. Total Environ.* **2021**, *754*, 142219. [CrossRef] [PubMed]
94. Song, S.L.; Zhang, H.H.; Han, S.; Xiao, S.S.; Du, Y.S.; Hu, K.; Wang, H.J.; Wu, C.D. Activation of persulfate by a water falling film DBD process for the enhancement of enrofloxacin degradation. *Chemosphere* **2022**, *301*, 134667. [CrossRef] [PubMed]
95. Ma, J.; Li, H.Y.; Chi, L.P.; Chen, H.K.; Chen, C.Z. Changes in activation energy and kinetics of heat-activated persulfate oxidation of phenol in response to changes in pH and temperature. *Chemosphere* **2017**, *189*, 86–93. [CrossRef] [PubMed]
96. Wen, D.; Li, W.T.; Lv, J.R.; Qiang, Z.M.; Li, M.K. Methylene blue degradation by the VUV/UV/persulfate process: Effect of pH on the roles of photolysis and oxidation. *J. Hazard. Mater.* **2020**, *391*, 121855. [CrossRef]
97. Shang, K.F.; Wang, X.J.; Li, J.; Wang, H.; Lu, N.; Jiang, N.; Wu, Y. Synergetic degradation of Acid Orange 7 (AO7) dye by DBD plasma and persulfate. *Chem. Eng. J.* **2017**, *311*, 378–384. [CrossRef]
98. Chen, W.G.; Wu, H.X.; Fan, J.W.; Fang, Z.; Lin, S.H. Activated persulfate by DBD plasma and activated carbon for the degradation of acid orange II. *Plasma Sci. Technol.* **2020**, *22*, 61–67. [CrossRef]
99. Wu, H.X.; Fan, J.W.; Liu, F.; Shu, L.S.; Yin, B.J. Degradation of tetracycline in aqueous solution by persulphate assisted gas-liquid dielectric barrier discharge. *Water Environ. J.* **2021**, *35*, 12678. [CrossRef]
100. Wang, Y.W.; Huang, J.W.; Guo, H.; Puyang, C.D.; Han, J.G.; Li, Y.; Ruan, Y.X. Mechanism and process of sulfamethoxazole decomposition with persulfate activated by pulse dielectric barrier discharge plasma. *Sep. Purif. Technol.* **2022**, *287*, 120540. [CrossRef]

101. Wu, J.L.; Xiong, Q.; Liang, J.L.; He, Q.; Yang, D.X.; Deng, R.Y.; Chen, Y. Degradation of benzotriazole by DBD plasma and peroxymonosulfate: Mechanism, degradation pathway and potential toxicity. *Chem. Eng. J.* **2022**, *384*, 123300. [CrossRef]
102. Tang, S.F.; Yuan, D.L.; Rao, Y.D.; Li, N.; Qi, J.B.; Cheng, T.Z.; Sun, Z.T.; Gu, J.M.; Huang, H.M. Persulfate activation in gas phase surface discharge plasma for synergetic removal of antibiotic in water. *Chem. Eng. J.* **2018**, *337*, 446–454. [CrossRef]
103. Liu, Y.; Qu, G.Z.; Sun, Q.H.; Jia, H.Z.; Wang, T.C.; Zhu, L.Y. Endogenously activated persulfate by non-thermal plasma for Cu (II)-EDTA decomplexation: Synergistic effect and mechanisms. *Chem. Eng. J.* **2021**, *406*, 126774. [CrossRef]
104. Wang, X.J.; Wang, P.; Liu, X.M.; Hu, L.M.; Wang, Q.; Xu, P.; Zhang, G.S. Enhanced degradation of PFOA in water by dielectric barrier discharge plasma in a coaxial cylindrical structure with the assistance of peroxymonosulfate. *Chem. Eng. J.* **2020**, *389*, 124381. [CrossRef]
105. Wang, B.W.; Wang, C.; Yao, S.M.; Peng, Y.P.; Xu, Y. Plasma-catalytic degradation of tetracycline hydrochloride over Mn/γ-Al_2O_3 catalysts in a dielectric barrier discharge reactor. *Plasma Sci. Technol.* **2019**, *21*, 136–143. [CrossRef]
106. Ma, H.; Yuan, C.C.; Wang, X.M.; Wang, H.J.; Long, Y.P.; Chen, Y.Q.; Wang, Q.; Cong, Y.Q.; Zhang, Y. Deposition of CeO_2 on TiO_2 nanorods electrode by dielectric barrier discharge plasma to enhance the photoelectrochemical performance in high chloride salt system. *Sep. Purif. Technol.* **2021**, *276*, 119252. [CrossRef]
107. Tang, S.F.; Lu, N.; Li, J.; Shang, K.F.; Wu, Y. Improved phenol decomposition and simultaneous regeneration of granular activated carbon by the addition of a titanium dioxide catalyst under a dielectric barrier discharge plasma. *Carbon* **2012**, *53*, 380–390. [CrossRef]
108. Wang, J.; Sun, Y.B.; Feng, J.W.; Xin, L.; Ma, J.Z. Degradation of triclocarban in water by dielectric barrier discharge plasma combined with TiO_2 /activated carbon fibers: Effect of operating parameters and byproducts identification. *Chem. Eng. J.* **2016**, *300*, 36–46. [CrossRef]
109. Wang, B.W.; Yao, S.M.; Peng, Y.P.; Xu, Y. Toluene removal over TiO_2-$BaTiO_3$ catalysts in an atmospheric dielectric barrier discharge. *J. Environ. Chem. Eng.* **2018**, *6*, 3819–3826. [CrossRef]
110. Wang, L.; Yu, Z.B.; Peng, Z.B.; Chen, Y.; Xiang, G.L.; Liu, Q.; Liu, Y.X.; Chen, D.M. Catalytic Properties of TiO_2/Fe_3O_4 Nanoparticles in Plasma Chemical Treatment. *Russ. J. Phys. Chem.* **2016**, *90*, 777–782. [CrossRef]
111. Shang, K.F.; Li, W.F.; Wang, X.J.; Lu, N.; Jiang, N.; Li, J.; Wu, Y. Degradation of p-nitrophenol by DBD plasma/Fe^{2+}/persulfate oxidation process. *Sep. Purif. Technol.* **2019**, *218*, 106–112. [CrossRef]
112. Deng, R.Y.; He, Q.; Yang, D.X.; Dong, Q.; Wu, J.L.; Yang, X.Y.; Chen, Y. Enhanced synergistic performance of nano-Fe^0-CeO_2 composites for the degradation of diclofenac in DBD plasma. *Chem. Eng. J.* **2021**, *406*, 126884. [CrossRef]
113. Zhao, L.; Hou, H.; Fujii, A.; Hosomi, M.; Li, F.S. Degradation of 1,4-dioxane in water with heat- and Fe $^{(2+)}$-activated persulfate oxidation. *Environ. Sci. Pollut. Res. Int.* **2014**, *21*, 7457–7465. [CrossRef] [PubMed]